

1 **Quantifying the role of moss in terrestrial ecosystem carbon dynamics in**
2 **northern high-latitudes**

3 Junrong Zha and Qianlai Zhuang

4 Department of Earth, Atmospheric, and Planetary Sciences and Department of Agronomy,
5 Purdue University, West Lafayette, IN 47907, USA

6 Correspondence: Qianlai Zhuang (qzhuang@purdue.edu)

7 To be submitted to: *Journal of Biogeoscience*

8 **Key words:** moss, carbon dynamics, Earth System Modeling, terrestrial ecosystems, Arctic

9

10

11

12

13

14

15

16

17

18

19 **Abstract**

20 **In addition to woody and herbaceous plants, mosses are ubiquitous in northern terrestrial**
21 **ecosystems, which play an important role in regional carbon, water and energy cycling.**
22 **Current global land surface models that do not considering moss may bias the**
23 **quantification of the regional carbon dynamics. Here we incorporate moss into a process-**
24 **based biogeochemistry model, the Terrestrial Ecosystem Model (TEM 5.0), as a new plant**
25 **functional type to develop a new model (TEM_Moss). The new model explicitly quantifies**
26 **the interactions between vascular plants and mosses and their competition for energy,**
27 **water, and nutrients. Compared to the estimates using TEM 5.0, the new model estimates**
28 **that the regional terrestrial soils store 132.7 Pg more C at present day, and will store 157.5**
29 **Pg and 179.1 Pg more C under the RCP 8.5 and RCP 2.6 scenarios, respectively, by the end**
30 **of the 21st century. Ensemble regional simulations forced with different parameters for the**
31 **21st century with TEM_Moss predict that the region will accumulate 161.1±142.1 Pg C**
32 **under the RCP 2.6 scenario, and 186.7±166.1 Pg C under the RCP 8.5 scenario over the**
33 **century. Our study highlights the necessity of coupling moss into Earth System Models to**
34 **adequately quantify terrestrial carbon-climate feedbacks in the Arctic.**

35

36

37

38

39

40 **1. Introduction**

41 Northern high latitude ecosystems, which refers to the land ecosystems (>45 °N) in
42 northern temperate, boreal, grassland and tundra regions, hold about 30% of global terrestrial
43 carbon (C) in soils and plants (Allison and Treseder, 2008; Jobbágy and Jackson, 2000;
44 Kasischke, 2000; Tarnocai et al., 2009; Hugelius et al., 2014), and contain as much as 1024 Pg
45 soil organic carbon from 0 to 3 m depth (Treseder et al., 2016; Schuur et al., 2008). This large
46 amount of carbon is potentially responsive to ongoing global warming (Burke et al., 2017,
47 Koven et al., 2015, Comyn-Platt et al., 2018)), which is especially pronounced at high latitudes
48 (Treseder et al., 2016; IPCC, 2014). Thus, explicit investigation of carbon-climate feedback is
49 important (Wieder et al., 2013; Bond-Lamberty and Thomson, 2010).

50 Ecosystem models are important tools for understanding the role of boreal ecosystems in
51 carbon-climate feedbacks (Bond-Lamberty et al., 2005; Chadburn et al., 2017; Zhuang et al.,
52 2002; Treseder et al., 2016). Process-based biogeochemical models such as TEM (Hayes et al.,
53 2014; Raich et al., 1991; Melillo et al., 1993; McGuire et al., 1992; Zhuang et al., 2001, 2002,
54 2010, 2013), Biome-BGC (Running and Coughlan, 1988; Bond-Lamberty et al., 2007), and
55 Biosphere Energy Transfer Hydrology scheme (BETHY) (Knorr, 2000) are increasingly
56 employed to simulate current and future carbon dynamics. Those models estimate carbon
57 dynamics by simulating processes such as photosynthesis, respiration, nitrogen competition,
58 evapotranspiration and soil decomposition (Bond-Lamberty et al., 2005; Zhuang et al., 2015).
59 The results from these models are influenced by components and processes that are built into the
60 model (Turetsky et al., 2012; Oreskes et al., 1994). However, the role of boreal forests in carbon
61 sink or source activities has not yet reached a consensus due to a number of model limitations
62 (Cahoon et al., 2012; Hayes et al., 2011; Todd-Brown et al., 2013).

63 One limitation is that ecosystems models often ignore some important components such
64 as understory processes that play crucial roles in biogeochemical cycles (Zhuang et al., 2002;
65 Treseder et al., 2011; Bond-Lamberty et al., 2005). For instance, mosses are ubiquitous in
66 northern ecosystems, and show a pattern of increasing abundance with increasing latitude
67 (Turetsky et al., 2012; Jägerbrand et al., 2006). Their functional traits, including tolerance to
68 drought and a broad response of net assimilation rates to temperature, allow them to persist in
69 high-latitude regions (Kallio and Heinonen, 1975; Harley et al., 1989). The activities of moss
70 that are related to water, nutrients, and energy may influence several ecosystem processes such
71 as permafrost formation and thaw, peat accumulation, soil decomposition and net primary
72 productivity (NPP) (Turetsky et al., 2012; Nilsson and Wardle, 2005). Mosses can have positive
73 or negative interactions with vascular plants (Skre and Oechel, 1979; Turetsky et al., 2010). On
74 the one hand, mosses compete with vascular plants for available nutrients, negatively affecting
75 vascular plants productivity (Skre and Oechel, 1979; Gornall et al., 2011; Turetsky et al., 2012).
76 Besides, a thick moss cover can form an environment with water logging or low oxygen supply,
77 which is common in high-latitude regions (Skre and Oechel, 1979; Cornelissen et al., 2007). The
78 moss cover prevents absorbed solar heat from being conducted down into the soil, and tends to
79 decrease soil temperature in summer. Therefore, soil decomposition rates can be affected since
80 they are mediated by soil temperature, which will further influence growth of vascular plants
81 (Gornall et al., 2007). On the other hand, some species of mosses can serve as an important
82 source of nitrogen because of their associations with microbial nitrogen fixers (Basilier, 1979;
83 DeLuca et al., 2007; Markham, 2009; Kip et al., 2011). Thus, mosses can also exert positive
84 effects on plant growth due to their regulation of nitrogen availability for vascular plants (Hobbie
85 et al., 2000; Gornall et al., 2007). It is gradually being recognized that mosses can have

86 comparable influences on high-latitude ecosystems to vascular plants, due to their large density
87 and essential function in plant competition, soil climate, and carbon and nutrient cycling
88 (Longton, 1988; Lindo and Gonzalez, 2010; Okland, 1995; Pharo and Zartman, 2007). They can
89 on average contribute 20% of aboveground NPP in boreal forests (Turetsky et al., 2010), and
90 their annual NPP may reach as high as 350 g C m⁻² in some regions in the Arctic (Pakarinen and
91 Vitt 1973), even exceeding that of vascular plants (Oechel and Collins, 1976; Clarke et al.,
92 1971). Thus, ignorance of mosses, the keystone species of boreal ecosystems, can pose large
93 biases in model predictions and limit the utility of models. To date, a number of ecosystem
94 models have already included moss activities to explore the response of moss to disturbance
95 (Bond-Lamberty et al., 2007; Euskirchen et al., 2009; Frohking et al., 2010, Wania et al., 2009,
96 Chadburn et al., 2015, Porada et al., 2016, Druel et al., 2017), or improve model prediction of
97 carbon dynamics (Bond-Lamberty et al., 2005). However, the potential role of moss in the
98 regional carbon dynamics in northern high latitudes has been slowly evaluated by considering
99 the interactions between moss and vascular plants, especially with respect to their competition
100 for water, nutrient and energy.

101 This study developed a new version of Terrestrial Ecosystem Model (Raich et al., 1991;
102 McGuire et al., 1992; Zhuang et al., 2001, 2002, 2010, 2013, 2015), hereafter referred to as
103 TEM_Moss, by explicitly considering moss impacts on terrestrial ecosystem carbon dynamics.
104 The competition of water, energy and nutrient between vascular plants and mosses are explicitly
105 modeled. The verified TEM_Moss and previous TEM were compared against the observed data of
106 ecosystem carbon, soil temperature and moisture dynamics. Both models were then used to analyze
107 the regional carbon dynamics in northern high latitudes (north of 45 °N) during the 20th and 21st
108 centuries.

109 **2. Methods**

110 **2.1 Overview**

111 First, we briefly describe how we developed the TEM_Moss by modifying the previous
112 TEM 5.0 to consider their interactions between vascular plants and mosses. Second,
113 parameterization and validation of TEM_Moss using measured gap-filled carbon flux data and
114 meteorological data at representative sites is presented. Third, we present how we have applied
115 both models (TEM_Moss and TEM 5.0) to the northern high latitudes (above 45 °N) to quantify
116 regional carbon dynamics during the 20th and 21st centuries.

117 **2.2 Model description**

118 TEM is a process-based, large-scale biogeochemical model that uses monthly climatic data
119 and spatially explicit vegetation and soil information to simulate the dynamics of carbon and
120 nitrogen fluxes and pool sizes of plants and soils (Raich et al., 1991; McGuire et al., 1992; Zhuang
121 et al., 2010, 2015, 2020). However, in previous versions of TEM, the interactions between mosses
122 and vascular plants on carbon and nitrogen cycling have not been included. Here we developed a
123 TEM_Moss model by modifying model structure and incorporating activities of moss into extant
124 TEM 5.0 (Zhuang et al., 2003). Based on the structure of TEM 5.0, we added carbon and nitrogen
125 pools and fluxes to simulate activities of moss including photosynthesis, respiration, litterfall and
126 nutrient and water cycling (Figure 1). Thus, the structure of TEM_Moss includes the processes of
127 both vascular plants and mosses (Figure 1).

128 In TEM_Moss, moss photosynthesis (GPP_m) is described as a maximum rate, reduced by
129 influence of photosynthetically active radiation, mean air temperature, mean atmospheric carbon

130 dioxide concentrations, moss moisture, and indirectly, nitrogen availability (Frolking et al., 1996;
131 Launiainen et al., 2015; Zhuang et al., 2002). For each time step, GPP_m is calculated as:

$$132 \quad GPP_m = C_{max} * f(PAR) * f(T) * f(w_m) * f([CO_2]) * f(NA) \quad (1)$$

133 where C_{max} denotes the maximum rate of carbon assimilation by moss (units: $gC\ m^{-2}mon^{-1}$),
134 $f(PAR)$ is a scalar function that depends on monthly photosynthetically active radiation (PAR),
135 which is calculated as (Frolking et al., 1996; Launiainen et al., 2015; Kulmala et al., 2011):

$$136 \quad f(PAR) = \frac{PAR}{b+PAR} \quad (2)$$

137 where b (units: $\mu mol\ m^{-2}\ s^{-1}$) is the half saturation constant for PAR use by moss as indicated by
138 the Michaelis–Menten kinetic.

139 The temperature effect on moss photosynthesis is modeled as a multiplier (Frolking et al.,
140 1996; Raich et al., 1991):

$$141 \quad f(T) = \frac{(T-T_{min})*(T-T_{max})}{(T-T_{min})*(T-T_{max})-(T-T_{opt})^2} \quad (3)$$

142 where T is the monthly mean air temperature (units: $^{\circ}C$), and T_{min} , T_{max} , and T_{opt} are parameters
143 (units: $^{\circ}C$) that limit $f(T)$ to a range of zero to one.

144 The moisture effect is also modeled as a multiplier (Frolking et al., 1996; Raich et al.,
145 1991):

$$146 \quad f(w_m) = \frac{(w_m-w_{min})*(w_m-w_{max})}{(w_m-w_{min})*(w_m-w_{max})-(w_m-w_{opt})^2} \quad (4)$$

147 where w_m is moss moisture (units: mm), and w_{min} , w_{max} , and w_{opt} are related parameters (units:
148 mm) that limit $f(w_m)$ to a range of zero to one.

149 $f([\text{CO}_2])$ is also a scalar function that depends on monthly mean atmospheric carbon
150 dioxide concentration (Zhuang et al., 2002; Raich et al., 1991):

$$151 \quad f([\text{CO}_2]) = \frac{[\text{CO}_2]}{k_m + [\text{CO}_2]} \quad (5)$$

152 where $[\text{CO}_2]$ (units: $\mu\text{L/L}$) represents monthly mean atmospheric carbon dioxide concentration,
153 the k_m (units: $\mu\text{L/L}$) is the internal CO_2 concentration at which moss C assimilation proceeds at
154 one-half its maximum rate.

155 The function $f(\text{NA})$ models the limiting effects of plant nitrogen status on GPP (McGuire
156 et al., 1992; Zhuang et al., 2002), which is a scalar function that depends on monthly N available
157 for incorporation into plant production of new tissue.

158 Meanwhile, in TEM_Moss, we defined the moss respiration rate (R_m) as a function of
159 moss respiration rate at 10 °C, moss respiration temperature sensitivity which was expressed as a
160 Q_{10} function, and moss moisture (Launiainen et al., 2015; Frohking et al., 1996):

$$161 \quad R_m = R_{10,m} * Q_{10,m}^{\frac{T_m - 10}{10}} * f^*(w_m) \quad (6)$$

162 where $R_{10,m}$ (units: $\text{gC m}^{-2}\text{mon}^{-1}$) represents the moss respiration rate at 10 °C, the parameter
163 $Q_{10,m}$ is moss respiration temperature sensitivity, T_m is moss temperature (°C) and w_m is moss
164 moisture (mm).

165 The function $f^*(w_m)$ denotes the moisture effect on moss respiration. Here we used
166 $f^*(w_m)$ to distinguish with the function $f(w_m)$, which is moisture effect on moss
167 photosynthesis as mentioned earlier. $f^*(w_m)$ is defined as (Frohking et al., 1996; Zhuang et al,
168 2002):

169
$$f^*(w_m) = 1 - \frac{(w_m - w_{\min} - w_{\text{opt},r})^2}{(w_m - w_{\min}) * w_{\text{opt},r} + w_{\text{opt},r}^2} \quad (7)$$

170 where $w_{\text{opt},r}$ (units: mm) denotes the optimal water content for moss respiration.

171 Besides, the carbon in litter production from mosses to soil ($L_{C,m}$) is modeled as
 172 proportional to moss carbon biomass with a constant ratio (Zhuang et al., 2002):

173
$$L_{C,m} = c_{\text{fall}_m} * \text{MOSSC} \quad (8)$$

174 where MOSSC denotes the moss carbon biomass, and c_{fall_m} is the corresponding constant
 175 proportion.

176 Thus, the change of moss carbon pool (MOSSC) can be modeled as:

177
$$\frac{d\text{MOSSC}}{dt} = \text{GPP}_m - R_m - L_{C,m} \quad (9)$$

178 On the other hand, researches have shown that mosses can uptake substantial inorganic
 179 nitrogen from the bulk soil (Ayres et al., 2006, Fritz et al., 2014). In our model, nitrogen uptake
 180 by moss (N_{uptake_m}) is modelled as a function of available soil nitrogen, moss moisture, and
 181 mean air temperature, and the relative amount of energy allocated to N versus C uptake (Zhuang
 182 et al., 2002; Raich et al., 1991):

183
$$N_{\text{uptake}_m} = N_{\text{max}} * \frac{K_s * N_{\text{av}}}{k_n + K_s * N_{\text{av}}} * e^{0.0693T} * (1 - A_m) \quad (10)$$

184 Where N_{max} is the maximum rate of nitrogen uptake by mosses (units: $\text{gC m}^{-2}\text{mon}^{-1}$), and N_{av}
 185 (units: g m^{-2}) represents available soil nitrogen, which is treated as a state variable in our model.
 186 k_n (units: g m^{-2}) is the concentration of available soil nitrogen at which nitrogen uptake proceeds
 187 at one-half its maximum rate. T is the monthly mean air temperature ($^{\circ}\text{C}$), and A_m is a unitless
 188 parameter ranging from 0 to 1, which represents relative allocation of effort to carbon vs.

189 nitrogen uptake. K_s is a parameter accounting for relative differences in the conductance of the
 190 soil to N diffusion, which can be calculated through moss moisture (Zhuang et al., 2002; Raich et
 191 al., 1991):

$$192 \quad K_s = 0.9 * \left(\frac{w_m}{w_f}\right)^3 + 0.1 \quad (11)$$

193 where w_f (units: mm) denotes the moss field capacity.

194 The nitrogen in litter production from mosses to soil ($L_{N,m}$) is modeled as proportional to
 195 moss nitrogen biomass with a constant ratio (Zhuang et al., 2002):

$$196 \quad L_{N,m} = nfall_m * MOSSN \quad (12)$$

197 where $nfall_m$ is the constant proportion to moss nitrogen biomass (MOSSN).

198 Thus, the changes in moss nitrogen pool (MOSSN) can be modeled as:

$$199 \quad \frac{dMOSSN}{dt} = Nuptake_m - L_{N,m} \quad (13)$$

200 At the same time, total carbon and nitrogen in litterfall, and total nitrogen uptake from
 201 soil available nitrogen are changed due to incorporation of mosses:

$$202 \quad Litterfall_C = L_{C,v} + L_{C,m} \quad (14)$$

$$203 \quad Litterfall_N = L_{N,v} + L_{N,m} \quad (15)$$

$$204 \quad Nuptake = Nuptake_v + Nuptake_m \quad (16)$$

205 Where $L_{C,v}$ and $L_{N,v}$ are carbon and nitrogen in litter production from vascular plants to soil, and
 206 $Nuptake_v$ is nitrogen uptake by vascular plants (Raich et al., 1991; Melillo et al., 1993; Zhuang
 207 et al., 2003).

208 Except above equations, other governing equations in TEM 5.0 have not been changed.
209 More equations of TEM 5.0 have been documented in previous studies (Raich et al., 1991;
210 McGuire et al., 1992; Zhuang et al., 2003; Zha and Zhuang, 2018).

211 In TEM 5.0, a soil thermal module (STM) simulates soil thermal dynamics considering
212 the effects of moss thickness, soil moisture, and snowpack (Zhuang et al., 2001, 2002). In STM,
213 soil profile was treated as a three soil-layer system: (1) a moss plus fibric soil organic layer, (2) a
214 humic organic soil layer, and (3) a mineral soil layer, and temperature for each layer can be
215 derived from STM (Zhuang et al., 2001, 2002, 2003). Temperature in moss layer is estimated
216 with STM.

217 A water balance module (WBM) was also incorporated into TEM 5.0 to simulate soil
218 hydrologic dynamics (Vörösmarty et al., 1989; Zhuang et al., 2001). The WBM receives
219 information on precipitation, air temperature, potential evapotranspiration, vegetation, soils and
220 elevation to predict soil moisture evapotranspiration and runoff (Vörösmarty et al., 1989). The
221 whole soil was treated as a single profile in WBM (Vörösmarty et al., 1989; Zhuang et al., 2001).
222 To simulate moss moisture, we added a moss layer on the soil profile by modifying the WBM
223 (Figure 2). Similar to soil moisture, moss moisture is also treated as a state variable in the revised
224 WBM, which is modeled as:

$$225 \quad \frac{dw_m}{dt} = \text{snowfall} + \text{rainfall} - \text{percolation} - \text{moss evapotranspiration} \quad (17)$$

226 where the term “percolation” denotes the percolation from moss, which is the sum of rainfall
227 percolation and snowmelt percolation from moss. We assume that there is no runoff from moss
228 layer.

229 Accompanied by the above equation, changes in soil water (SM) is modified as:

230
$$\frac{dSM}{dt} = \text{percolation} - \text{rain excess} - \text{snow excess} - \text{plant evapotranspiration} \quad (18)$$

231 Calculations for these water fluxes regarding vascular plants were not changed. More details
232 about an earlier version of WBM were described in Vörösmarty et al. (1989) and Zhuang et al.
233 (2001).

234 **2.3 Model parameterization and validation**

235 The newly introduced parameters that are associated with moss activities were documented
236 in Table 1. We parameterized the TEM_Moss for six representative ecosystem types in northern
237 high latitudes with gap-filled monthly net ecosystem productivity (NEP, $\text{gCm}^{-2}\text{mon}^{-1}$) data from
238 the AmeriFlux network (Davidson et al., 2000). We assumed that the moss types are associated
239 with the representative ecosystem types, which means we tuned the moss-related parameters for
240 the six representative ecosystem types. Except for the moss-related parameters, other parameters
241 related to vascular plants are default based on Zha and Zhuang, 2018. The information of six sites
242 that we chose to calibrate the TEM_Moss was compiled in Table 2. The parameterization was
243 conducted using a global optimization algorithm known as SCE-UA (Shuffled complex evolution)
244 method, which aims to minimize the difference between model simulations and measurements
245 (Duan et al., 1994). In our calibration, the cost function of the minimization is:

246
$$\text{Obj} = \sum_{i=1}^k (\text{NEP}_{\text{obs},i} - \text{NEP}_{\text{sim},i})^2 \quad (19)$$

247 Where $\text{NEP}_{\text{obs},i}$ and $\text{NEP}_{\text{sim},i}$ are the measured and simulated NEP, respectively. k is the number
248 of data pairs for comparison. Fifty independent sets of parameters were converged to minimize the
249 objective function, and finally the optimized parameters were derived as the mean of these 50 sets
250 of inversed parameters. We presented the boxplot of parameter posterior distributions at sites
251 chosen for calibration (Figure 5). At the same time, the results of model parameterization were

252 shown in Figure 3. Besides these parameters related to moss, all other parameters use their default
253 values in TEM 5.0 (Zhuang et al., ~~2003~~2019). Note, in TEM 5.0 and its application, the parameters
254 were also calibrated for each representative ecosystem in northern high latitudes. Specifically,
255 TEM 5.0 was parameterized for mixed grassland/sub-shrublands, moist non-acidic tundra, mixed
256 hardwood and conifer forests, tallgrass prairie, savanna tropical forests, tussock tundra, and conifer
257 forest in the region. TEM 5.0 was then extrapolated to the region to quantify carbon dynamics
258 without considering the role of moss in boreal ecosystems (Zhuang et al., 2003). Here our revised
259 model TEM_Moss was parameterized for representative ecosystems in the region by explicitly
260 considering the role of moss in soil physics and carbon and nitrogen dynamics. These TEM_Moss
261 optimized parameters were then used for model validation and extrapolation—as well as
262 comparison with TEM 5.0 simulations.

263 We verified the TEM_Moss simulated NEP, soil moisture and soil temperature. First, we
264 conducted site-level simulations at six sites that contain level-4 gap-filled monthly NEP data from
265 the AmeriFlux network (Table 3). Site-level monthly gap-filled soil moisture and soil temperature
266 data were organized from the ORNL DAAC Dataset (<https://daac.ornl.gov/>) to make comparison
267 with model simulations (Table 4 and Table 5). Local climate data including monthly air
268 temperature (°C), precipitation (mm), and cloudiness (%) were obtained to drive these model
269 simulations.

270 **2.4 Regional Extrapolation**

271 With six site-level calibrated parameters, TEM-Moss is applied to the region pixel by pixel based
272 on vegetation distribution data. Both TEM_Moss and TEM 5.0 were applied to northern high
273 latitudes (above 45°N) for historical (the 20th century) and future (the 21st century) quantifications
274 on carbon dynamics. For historical simulations, climatic forcing data including monthly air

275 temperature, precipitation, and cloudiness and atmospheric CO₂ concentrations during the 20th
276 century, were collected from the Climatic Research Unit (CRU TS3.1) from the University of East
277 Anglia (Harris et al., 2014). Other ancillary inputs including gridded soil texture (Zhuang et al.,
278 2015), elevation (Zhuang et al., 2015), and potential natural vegetation (Melillo et al., 1993) were
279 also organized. For future simulations, two contrasting Intergovernmental Panel on Climate
280 Change (IPCC) climate scenarios (RCP 2.6 and RCP 8.5) were used to drive the models. The future
281 climate forcing data and atmospheric CO₂ concentrations during the 21st century under these two
282 climate change scenarios were derived from the HadGEM2-ESmodel, which is a member of
283 CMIP5project213 (<https://esgf-node.llnl.gov/search/cmip5/>, January 2017).

284 Simulations were conducted at a spatial resolution of 0.5° latitude × 0.5° longitude (Zhuang
285 et al., 2001, 2002). A spin-up was run to reach an equilibrium for each pixel, and the values of state
286 variables at equilibrium were treated as initial values for transient simulations (McGuire et al.,
287 1992). Specifically, we chose the first 30 years in the whole 100-year climatic forcing data to spin-
288 up the models when conducting historical and future simulations. For each of the simulations, net
289 primary production (NPP), heterotrophic respiration (R_H), and net ecosystem production (NEP)
290 were analyzed. We denoted that a positive NEP represents a CO₂ sink from the atmosphere to
291 terrestrial ecosystems, while a negative value represents a source of CO₂ from terrestrial
292 ecosystems to the atmosphere.

293 In these simulations, for each pixel, we assumed its moss distribution area is the same as
294 the vascular plant distribution. The total carbon uptake/emission of mosses in a pixel are calculated
295 as the multiplication of pixel area with the carbon fluxes such as NEP (units: gC m⁻² month⁻¹).
296 Moss-related parameters for representative ecosystems are calibrated (Fig. 4 and Table 1) or

297 obtained from previous model parameterization and the rest of model parameters are default from
298 Zha and Zhuang (2018).

299 **3. Results**

300 **3.1 Model Validation**

301 TEM_Moss was able to reproduce the monthly NEP and performed better than TEM 5.0
302 at chosen sites, with larger R-square values and smaller RMSE (Figure 6, Table 6). R-square for
303 TEM_Moss reached 0.94 at Bartlett Experimental Forest site and 0.72 at Ivotuk site (Table 6). R-
304 square values for TEM 5.0 showed a similar pattern, reaching 0.91 and with minimum value of
305 0.43 at Bartlett Experimental Forest and Ivotuk sites, respectively (Table 6). Except for Ivotuk
306 site, R-squares for TEM_Moss are all higher than 0.8 at the chosen sites, while most R-squares
307 for TEM 5.0 are from 0.62 to 0.75 (Table 6). On the other hand, RMSE for TEM_Moss is lower
308 than that for TEM 5.0 at each site (Table 6).

309 We presented the comparisons between measured and simulated volumetric soil moisture
310 (VSM) from TEM_Moss and TEM 5.0 (Figure 7). Statistical analysis shows that TEM_Moss
311 reproduces the soil moisture well with R-squares ranging from 0.51 at US-Bkg to 0.87 at US-Atq
312 (Table 7). R-squares for TEM_Moss are substantially higher than that for TEM 5.0 at most
313 chosen sites, except for US-Atq (Table 7). RMSE for TEM_Moss is lower than that for TEM 5.0
314 at each site (Table 7). Similarly, comparisons between measured and simulated soil temperature
315 at 5 cm depth (ST_5) from TEM_Moss and TEM 5.0 indicated that TEM_Moss can reproduce
316 the soil temperature with R-squares ranging from 0.81 at US-Ho1 to 0.91 at US-Bkg, while TEM
317 5.0 reproduces the soil temperature with R-squares ranging from 0.69 at BE-Vie to 0.89 at US-
318 Bkg (Figure 8; Table 8). Although R-squares for both models are relatively high and RMSE for

319 them are relatively low, TEM_Moss still shows higher R-squares and lower RMSE than TEM
320 5.0 (Table 8).

321 **3.2 Regional carbon dynamics during the 20th century**

322 Both TEM_Moss and TEM 5.0 were used to simulate northern high-latitude regional
323 carbon balance during the 20th century (Figure 9). Higher NEP was correlated with the
324 combination of relatively higher NPP and lower heterotrophic respiration (R_H). TEM_Moss
325 indicated that the northern high latitudes acted as a carbon sink of 221.9 Pg with an inter-annual
326 standard deviation of 0.31 PgC yr⁻¹ during the 20th century, which is 132.7 Pg larger than 89.2 Pg
327 simulated by TEM 5.0 (Figure 10). The simulated NEP by TEM_Moss ranges from 1.38 PgC yr⁻¹
328 to 3.05 PgC yr⁻¹, while the range by TEM 5.0 was from 0.11 PgC yr⁻¹ to 1.75 PgC yr⁻¹ (Figure 9).
329 The patterns of the simulated NEP from two models were similar, both showing a general
330 increasing trend throughout the 20th century (Figure 9). By 2000, the TEM_Moss simulation
331 indicated that the northern high-latitude region stored 3.05 PgC yr⁻¹, which is more than twice as
332 the storage estimated by TEM 5.0 (1.33 PgC yr⁻¹, Figure 9). Both models indicated that carbon
333 uptake by the northern ecosystems during the second half of the 20th century was higher than the
334 first half for most part of the region, and only a small portion of the region lost carbon in last
335 century (Figure 10).

336 Simulated total NPP by TEM_Moss was 9.6 PgC yr⁻¹, ranging from 8.52 PgC yr⁻¹ to
337 10.65 PgC yr⁻¹ in the 20th century, with 1.69 PgC yr⁻¹ of moss NPP and 7.93 PgC yr⁻¹ of vascular
338 plants NPP (Figure 9). Moss NPP ranges from 1.23 PgC yr⁻¹ to 2.14 PgC yr⁻¹ and the ratio of
339 moss NPP to vascular plants NPP is 0.21 (Figure 9). TEM 5.0 estimated 0.8 PgC yr⁻¹ lower total
340 NPP than TEM_Moss, but 0.87 PgC yr⁻¹ higher NPP for vascular plants (Figure 9). On the other
341 hand, average heterotrophic respiration in the 20th century was 7.38 PgC yr⁻¹ and all years were

342 within about 5% of this value (Figure 9). TEM 5.0 projected 0.53 PgC yr⁻¹ higher R_H than
343 TEM_Moss (7.91 PgC yr⁻¹, Figure 9). Overall, TEM_Moss predicted higher total NPP but lower
344 R_H, which jointly caused a pronounced difference in NEP between two models.

345 Both models estimated that soil organic carbon and vegetation carbon were accumulating
346 continuously in the 20th century (Figure 11). TEM_Moss indicated that regional SOC and VEGC
347 accumulated 96.3 PgC and 115.2 PgC, respectively, and the carbon uptake by moss was 10.4 Pg in
348 the period (Figure 11, Table 10). As simulated by TEM_Moss, 43.4%, 51.9% and 4.7% of total
349 carbon uptake in the region was assimilated to soils, vascular plants and mosses, respectively
350 (Table 10). TEM 5.0 simulated that SOC increased by 31.7 Pg at the end of the 20th century,
351 which is 64.6 PgC less than the value estimated by TEM_Moss (Table 10). TEM 5.0 estimated
352 57.7 PgC in plants less than the value estimated by TEM_Moss (57.5 PgC, Table 10). 35.5% and
353 64.5% of total carbon was as SOC and VEGC, respectively.

354 **3.3 Regional carbon dynamics during the 21st century**

355 Under the RCP 2.6 scenario, TEM_Moss simulated NEP of 2.07 PgC yr⁻¹ with the range
356 from 0.41 PgC yr⁻¹ to 3.2 PgC yr⁻¹, and the inter-annual standard deviation of 0.59 PgC yr⁻¹
357 during the 21st century (Figure 12 (a)). The regional sink shows a decreasing pattern in the 2000s
358 and then generally increases over the remaining years of the 21st century (Figure 12 (a)). For
359 comparison, TEM 5.0 predicted that the average NEP of 0.28 PgC yr⁻¹ with the range from -1.48
360 PgC yr⁻¹ to 1.69 PgC yr⁻¹ during the 21st century (Figure 12 (a)). Thus, TEM 5.0 projected 179.1
361 PgC stored in northern ecosystems is less than the estimation from TEM_Moss in the 21st
362 century. Besides, TEM 5.0 simulated that the regional NEP showed a decreasing trend and the
363 region fluctuates between sinks and sources during the century (Figure 12 (a)). The spatial
364 patterns from two models also showed differences. TEM_Moss indicated that the region

365 accumulates carbon over this century, while TEM 5.0 simulated that some regions changed from
366 a carbon sink to a source in the second half of the century (Figure 13 (a)). Simulated regional
367 NPP by TEM_Moss ranges from 11.2 to 13.7 PgC yr⁻¹ with a mean of 12.98 PgC yr⁻¹ in this
368 century, while average NPP predicted by TEM 5.0 is 1.46 PgC yr⁻¹ lower than that value (11.52
369 PgC yr⁻¹ (Figure 12(a)). TEM_Moss simulated NPP has 3.74 PgC yr⁻¹ from moss and 9.24 PgC
370 yr⁻¹ from vascular plants, which account for 28.8% and 71.2% of total NPP, respectively (Figure
371 12(a)). Meanwhile, TEM_Moss estimated that R_H is 10.91 PgC yr⁻¹, while TEM 5.0 predicted it
372 as 11.24 PgC yr⁻¹, which is higher (Figure 12(b)). Both models projected that soil organic
373 carbon and vegetation carbon accumulate in this century but with different magnitudes (Figure
374 14 (a)). TEM_Moss predicted that regional SOC and VEGC accumulated 84.7 PgC and 112.6
375 PgC, respectively, during the 21st century, while TEM 5.0 predicted that a smaller increase with
376 12.1 and 15.5 PgC in SOC and VEGC, respectively (Figure 14 (a), Table 12 (a)). Besides,
377 TEM_Moss also predicted an increasing of 9.4 PgC in MOSSC, accounting for 4.5% of the total
378 carbon uptake in this region (Table 12(a)).

379 Under the RCP 8.5 scenario, TEM_Moss simulated annual NPP of 13.84 PgC yr⁻¹ with a
380 range from 11.09 to 16.94 PgC yr⁻¹, which is 1.31 PgC yr⁻¹ higher than the projection from TEM
381 5.0 (Figure 12 (b)). Total NPP estimated by TEM_Moss has 3.84 PgC yr⁻¹ from moss and 10
382 PgC yr⁻¹ from vascular plants (Figure 12(b)). Annual R_H was 11.28 PgC yr⁻¹ estimated by
383 TEM_Moss and 11.54 PgC yr⁻¹ by TEM 5.0, respectively (Figure 12(b)). Consequently,
384 TEM_Moss projected NEP was 2.56 PgC yr⁻¹ with the inter-annual standard deviation of 0.93
385 PgC yr⁻¹ in this century (Figure 12(b)). NEP ranges from 0.67 PgC yr⁻¹ to 4.78 PgC yr⁻¹
386 estimated with TEM_Moss, while from -1.69 PgC yr⁻¹ to 2.65 PgC yr⁻¹ with a mean of 0.99 PgC
387 yr⁻¹ was estimated by TEM 5.0 (Figure 12(b)). TEM_Moss predicted more carbon uptake of

388 157.5 Pg than TEM 5.0 during the 21st century. Both models predicted that NEP showed an
389 increasing trend during the 21st century (Figure 12(b)). Moreover, similar spatial patterns of
390 carbon sinks and sources appeared in the projections from two models (Figure 13(b)). Soil
391 organic carbon and vegetation carbon shows an increasing trend from both models (Figure
392 14(b)). Regional SOC and VEGC increased by 92.5 PgC and 153.6 PgC, respectively by the end
393 of the 21st century predicted by TEM_Moss. In contrast, the increase of 44.2 PgC and 54.5 PgC of
394 SOC and VEGC, respectively, was predicted by TEM 5.0 (Figure 14(b), Table 12 (b)). TEM_Moss
395 predicted an increase of 10.1 PgC in MOSSC (Table 12(b)).

396 **4. Discussion**

397 **4.1 The role of moss in the regional carbon dynamics**

398
399 Global warming has been pronounced in recent decades, particularly at high latitudes
400 (IPCC, 2014; Tape et al., 2006; Stow et al., 2004). An enormous amount of soil organic carbon
401 stored in northern high-latitude regions (Tarnocai et al., 2009; Schuur et al., 2008) is expected to
402 affect a broad spectrum of ecological and human systems, and cause rapid changes in the Earth
403 system when undergoing substantial climate change (Serreze and Francis 2006; Davidson and
404 Janssens, 2006; McGuire et al., 2009). Improving projections for carbon budget of high latitude
405 terrestrial ecosystems is essential for understanding global carbon–climate feedbacks (Melillo et
406 al., 2011; Todd-Brown et al., 2013).

407 Our simulations suggest that mosses play an important role in the regional carbon
408 dynamics, which is consistent with previous studies (McGuire et al., 2009; Turetsky et al., 2012).
409 First of all, mosses are productive with carbon assimilation even during low temperature, water
410 content and irradiance (Kallio and Heinonen, 1975; Harley et al., 1989). For example, mosses
411 can tolerate drought through physiological responses, such as by suspending metabolism and by

412 withstanding cell desiccation (Turetsky et al., 2012; Oechel and Van Cleve, 1986). The key
413 functional traits related to water, nutrient, and thermal tolerances of mosses enable them to fit in
414 harsh northern conditions (Shetler et al., 2008; Turetsky et al., 2012). Thus, with incorporation of
415 moss into our models, the total NPP estimation in our model is affected. Mosses also act as a
416 powerful competitor with vascular plants for nutrient uptake. Their rapid nutrient acquisition and
417 slow nutrient loss through slow decomposition may constrain concentrations of plant-available
418 nitrogen (Hobbie et al., 2000; Turetsky et al., 2010; Oechel and Van Cleve, 1986; Gornall et al.,
419 2007), which will further decrease NPP of vascular plants. Our model results suggested that the
420 NPP of vascular plants considering moss is indeed lower than previous NPP estimates without
421 considering moss, but the total NPP is larger than before. We estimated that mosses contribute
422 17.6% of NPP in the 20th century, and 28.8% and 27.6% in the 21st century under the RCP 2.6
423 and RCP 8.5 scenarios, respectively. This is comparable with the results reported by a synthesis
424 study, indicating an average contribution 20% of aboveground NPP from moss in upland boreal
425 forests and the contribution is 48% in wetlands ecosystems. Frohking et al. (1996) even reported
426 a contribution of 38.4% to total NPP by moss at a boreal forest site. Moreover, mosses can also
427 influence heterotrophic respiration (R_H) through their effects on soil thermal and hydrologic
428 dynamics (Zhuang et al., 2001). With the layer of moss, soil temperature tends to decrease but
429 soil moisture tends to increase (Oechel and Van Cleve, 1986), which will further decrease soil
430 respiration in summer. This supports our results that TEM_Moss simulated R_H is lower than that
431 by TEM 5.0. With a combination of higher NPP and lower R_H , NEP predicted by TEM_Moss is
432 larger than that by TEM 5.0. The two contrasting regional simulations by TEM_Moss and TEM
433 5.0 indicated the region is currently a carbon sink, which is consistent with previous studies
434 (White et al., 2000; McGuire et al., 2009; Schimel et al., 2001). Our study estimates that regional

435 NEP during the 20th century is 2.2 Pg C yr⁻¹ by TEM_Moss and 0.89 Pg C yr⁻¹ by TEM 5.0,
436 respectively. In the 1990s, the regional sink is projected to be 2.7 and 1.1 Pg C yr⁻¹ by
437 TEM_Moss and TEM 5.0 respectively. Compared with other existing studies, our regional
438 estimates of NEP are within the reasonable range from other existing studies. McGuire et al.
439 (2009) estimated a land sink of 0.3–0.6 Pg C yr⁻¹ for the pan-arctic region for the 1990s, which is
440 closer to our estimation by TEM 5.0 but less than the projection by TEM_Moss. The top-down
441 atmospheric analyses indicate that the sink of pan-arctic region is between 0 and 0.8 Pg C yr⁻¹ in
442 the 1990s (Menon et al. 2007). Besides, Schimel et al. (2001) reported an estimation of the
443 northern extratropical NEP is from 0.6 to 2.3 PgC yr⁻¹ in the late 20th century, which is
444 comparable to our estimates. Our simulations also confirmed that mosses and vascular plants
445 respond to climate change similarly in terms of their productivity (Turetsky et al. 2010).

446 **4.2 Model Uncertainty and limitations**

447 There are a number of uncertainty sources in our model simulations. First, due to the
448 limited understanding of moss photosynthesis (He et al., 2015) and various moss N uptake
449 pathways (e.g., Bay et al 2013; Berg et al 2013), a few important assumptions have been made in
450 our modeling. For instance, we assume that mosses behave similarly to vascular plants regarding
451 photosynthesis and soil N uptake is the only pathway for mosses without considering N uptake
452 through N fixers and atmospheric wet N deposition (Ayres et al. 2006). Second, the errors in the
453 observed data will influence our parameterization results, which will bias our regional estimates
454 of carbon dynamics. Second, climatic driving data are also a source of uncertainty for historical
455 and future simulations. Third, model assumptions will also induce additional uncertainties. For
456 instance, we assumed that vegetation distribution will remain unchanged during the transient
457 simulation. However, vegetation will change in response to warming climate and disturbances

458 such as fire and insect outbreaks in the region (Hansen et al., 2006), which will affect carbon
459 budget. Missing potential responses to disturbances in our model shall introduce additional
460 uncertainties (Soja et al. 2007; Kasischke and Turetsky, 2006). Future moss dynamics will also
461 impact carbon dynamics in this region. For instance, a long-term warming experiments along
462 natural climatic gradients, ranging from Swedish subarctic birch forest and subarctic/subalpine
463 tundra to Alaskan arctic tussock tundra concluded that both diversity and abundance of mosses
464 are likely to decrease under arctic climate warming (Long et al. 2012). Similarly, total moss
465 cover declined in both heath and mesic meadow under experimental long-term warming (by 1.5–
466 3 °C), driven by general declines in many species (Alatalo et al., 2020). Due to global warming,
467 significant losses in moss diversity are expected in boreal forests and alpine biomes, leading to
468 changes in ecosystem structure and function, nutrient cycling, and carbon balance (He et al.,
469 2015).

470 We conducted ensemble regional simulations with 50 sets of parameters to quantify
471 model uncertainty due to uncertain parameters. The 50 sets of parameters were obtained using
472 the method in Tang and Zhuang (2008). The ensemble means and the inter-simulation standard
473 deviations are used to measure the model uncertainty (Figure 15). TEM_Moss predicted that the
474 regional cumulative carbon ranges from a carbon loss of 266 Pg C to a carbon sink of 567.3 Pg C
475 by different ensemble members, with a mean of 161.1 ± 142.1 Pg during the 21st century under the
476 RCP 2.6 scenario. Under the RCP 8.5 scenario, TEM_Moss predicted that the region acts from a
477 carbon source of 79.1 Pg C to a carbon sink of 625.9 Pg C, with a mean of 186.7 ± 166.1 Pg
478 during the 21st century (Figure 15).

479 This study took an important step to incorporate moss into an extant ecosystem model
480 that has not explicitly consider the role of moss and its interactions with vascular plants. Our

481 model simulations showed that mosses have strong influences on regional ecosystem carbon
482 cycling, by affecting the soil thermal, nitrogen availability, and water conditions of terrestrial
483 ecosystems. However, there are still limitations in our model. First, we did not differentiate
484 various kinds of mosses because they have their own functional traits. Different kinds of mosses
485 may provide different levels of insulation for soil, resulting in different soil thermal conditions
486 that affect microbial activities. The structural and physiological traits of mosses will differ
487 largely in different moss groups, such as feather moss versus Sphagnum (Turetsky et al., 2010).
488 In addition, we lack spatially explicit information of moss distribution in the region, which will
489 lead to a large regional uncertainty of carbon quantification. We assumed that moss area
490 distribution is the same as its associated vegetation distribution. Another limitation is that some
491 important physiological traits of moss have not been modeled. For example, moss abundance
492 may change following shifts in vascular species composition due to shading or burial by vascular
493 litter (Turetsky et al., 2010; Cornelissen et al., 2007). Furthermore, disturbance such as wildfires
494 can also influence moss activities.

495 **5. Conclusions**

496 This study explicitly incorporated moss into an extant process-based terrestrial ecosystem model
497 to investigate the carbon dynamics in the Arctic for present day and future. Historical regional
498 simulations with TEM_Moss indicated that the region is a carbon sink of 221.9 PgC over the 20th
499 century, and this sink may decrease to 206.7 PgC under the RCP 2.6 scenario or increase to 256.2
500 PgC under the RCP 8.5 scenario during the 21st century. Compared with an earlier version of TEM
501 that has not explicitly modeled moss, TEM_Moss projected that the region stored 132.7 Pg more
502 C over the last century, 179.1 Pg and 157.5 Pg more C under the RCP 2.6 and RCP 8.5 scenarios,
503 respectively. This study demonstrated that moss activities have large effects on ecosystem soil

504 thermal, water, and carbon dynamics through their interactions with vascular plants. This study
505 highlights the importance of considering the moss dynamics in Earth System Models to adequately
506 quantify the carbon–climate feedbacks in the Arctic.

507 **6. Acknowledgments**

508 This research was supported by an NSF project (IIS-1027955), a DOE project (DE-SC0008092),
509 and a NASA LCLUC project (NNX09AI26G). We acknowledge the Rosen High Performance
510 Computing Center at Purdue for computing support. We also acknowledge the World Climate
511 Research Programme’s Working Group on Coupled Modeling Intercomparison Project CMIP5,
512 and we thank the climate modeling groups for producing and making available their model
513 output. The data of this study can be accessed from Purdue Research Repository.

514

515 **References**

- 516 Allison, S. D., and Treseder, K. K.: Warming and drying suppress microbial activity and carbon cycling in
517 boreal forest soils, *Global change biology*, 14, 2898-2909, 10.1111/j.1365-2486.2008.01716.x, 2008.
- 518 Basilier, K.: Moss-associated nitrogen fixation in some mire and coniferous forest environments around
519 Uppsala, Sweden, *Lindbergia*, 5, 84-88, 1979.
- 520 Bay, G., Nahar, N., Oubre, M., Whitehouse, M.J., Wardle, D.A., Zackrisson, O., Nilsson, M.-C. and
521 Rasmussen, U. (2013), Boreal feather mosses secrete chemical signals to gain nitrogen. *New Phytol*, 200:
522 54-60. <https://doi.org/10.1111/nph.12403>
- 523 Ben Bond-Lamberty, S. T. G., Douglas E. Ahl and Peter E. Thornton: Reimplementation of the Biome-
524 BGC model to simulate successional change, *Tree Physiology*, 25, 413–424, 2005.
- 525 Berg, Andreas, et al. “Transfer of Fixed-N from N₂-Fixing Cyanobacteria Associated with the Moss
526 Sphagnum Riparium Results in Enhanced Growth of the Moss.” *Plant and Soil*, vol. 362, no. 1/2, 2013,
527 pp. 271–278. JSTOR, www.jstor.org/stable/42951898. Accessed 28 May 2021.
- 528 Bond-Lamberty, B., Peckham, S. D., Ahl, D. E., and Gower, S. T.: Fire as the dominant driver of central
529 Canadian boreal forest carbon balance, *Nature*, 450, 89-92, 10.1038/nature06272, 2007.
- 530 Bond-Lamberty, B., and Thomson, A.: Temperature-associated increases in the global soil respiration
531 record, *Nature*, 464, 579-582, 10.1038/nature08930, 2010.

532 Burke, E. J., Ekici, A., Huang, Y., Chadburn, S. E., Huntingford, C., Ciais, P., Friedlingstein, P., Peng, S.
533 & Krinner, G. 2017. Quantifying uncertainties of permafrost carbon-climate feedbacks. *Biogeosciences*,
534 14, 3051-3066.

535 Cahoon, S. M., Sullivan, P. F., Shaver, G. R., Welker, J. M., Post, E., and Holyoak, M.: Interactions
536 among shrub cover and the soil microclimate may determine future Arctic carbon budgets, *Ecology*
537 letters, 15, 1415-1422, 10.1111/j.1461-0248.2012.01865.x, 2012.

538 Chadburn, S. E., Burke, E. J., Cox, P. M., Friedlingstein, P., Hugelius, G., and Westermann, S.: An
539 observation-based constraint on permafrost loss as a function of global warming, *Nature Climate Change*,
540 7, 340-344, 10.1038/nclimate3262, 2017.

541 Charles J. Vörösmarty, B. M. I., Annette L. Grace, and M. Patricia Gildea: Continental scale models of
542 water balance and fluvial transport: an application to South America, *Global biogeochemical cycles*, 3,
543 241-265, 1989.

544 Christian Fritz, L. P. M. L., Muhammad Riaz, Leon J. L. van den Berg, Theo J. T.M. Elzenga: Sphagnum
545 Mosses - Masters of Efficient N-Uptake while Avoiding Intoxication, *PLoS ONE*, 9,
546 10.1371/journal.pone.0079991, 2014.

547 Clarke, G. C. S.: Productivity of Bryophytes in Polar Regions, *Annals of botany*, 35, 99–108, 1971.

548 Collins, W. C. O. a. N. J.: Comparative CO₂ exchange patterns in mosses from two tundra habitats at
549 Barrow, Alaska, *Canadian Journal of Botany*, 54, 1355-1369, 1976.

550 Comyn-Platt, E., Hayman, G., Huntingford, C., Chadburn, S. E., Burke, E. J., Harper, A. B., Collins, W.
551 J., Webber, C. P., Powell, T., Cox, P. M., Gedney, N. & Sitch, S. 2018. Carbon budgets for 1.5 and 2 °C
552 targets lowered by natural wetland and permafrost feedbacks. *Nature Geoscience*, 11, 568-573.

553 Cornelissen, J. H., Lang, S. I., Soudzilovskaia, N. A., and During, H. J.: Comparative cryptogam ecology:
554 a review of bryophyte and lichen traits that drive biogeochemistry, *Annals of botany*, 99, 987-1001,
555 10.1093/aob/mcm030, 2007.

556 Davidson, E. A., Trumbore, S. E., and Amundson, R.: Soil warming and organic carbon content, *Nature*,
557 408, 789, 10.1038/35048672, 2000.

558 Davidson, E. A., and Janssens, I. A.: Temperature sensitivity of soil carbon decomposition and feedbacks
559 to climate change, *Nature*, 440, 165-173, 10.1038/nature04514, 2006.

560 Davidson, E. A., Janssens, I. A., and Luo, Y.: On the variability of respiration in terrestrial ecosystems:
561 moving beyond Q₁₀, *Global change biology*, 12, 154-164, 10.1111/j.1365-2486.2005.01065.x, 2006.

562 DeLuca, T. H., Zackrisson, O., Gentili, F., Sellstedt, A., and Nilsson, M. C.: Ecosystem controls on
563 nitrogen fixation in boreal feather moss communities, *Oecologia*, 152, 121-130, 10.1007/s00442-006-
564 0626-6, 2007.

565 Duan, Q., Sorooshian, S., and Gupta, V. K.: Optimal use of the SCE-UA global optimization method for
566 calibrating watershed models, *Journal of Hydrology*, 158, 265-284, 1994.

567 E. S. Euskirchen, A. D. M., F. S. Chapin, III, S. Yi, and C. C. Thompson: Changes in vegetation in
568 northern Alaska under scenarios of climate change, 2003–2100: implications for climate feedbacks,
569 *Ecological Applications*, 19, 1022–1043, 2009.

570 Edward A. G. Schuur, J. B., Josep G. Canadell, Eugenie Euskirchen, Christopher B., Field, S. V. G.,
571 Stefan Hagemann, Peter Kuhry, Peter M. Lafleur, Hanna Lee, Galina, Mazhitova, F. E. N., Annette Rinke,
572 Vladimir E. Romanovsky, Nikolay Shiklomanov, and Charles Tarnocai, S. V., Jason G. Vogel, And Sergei
573 A. Zimov: Vulnerability of Permafrost Carbon to Climate Change: Implications for the Global Carbon
574 Cycle, *BioScience*, 58, 701-714, 2008.

575 Edward Ayres, R. v. d. W., Martin Sommerkorn, Richard D. Bardgett: Direct uptake of soil nitrogen by
576 mosses, *Biology Letters*, 2, 286-288, 10.1098/rsbl.2006.0455, 2006.

577 Esteban G. Jobbágy, and Jackson, R. B.: The vertical distribution of soil organic carbon and its relation to
578 climate and vegetation, *Ecological applications*, 10, 423-436, 2000.

579 Frolking, S., Roulet, N. T., Tuittila, E., Bubier, J. L., Quillet, A., Talbot, J., and Richard, P. J. H.: A new
580 model of Holocene peatland net primary production, decomposition, water balance, and peat
581 accumulation, *Earth System Dynamics*, 1, 1-21, 10.5194/esd-1-1-2010, 2010.

582 Gilmanov, T. G., Tieszen, L. L., Wylie, B. K., Flanagan, L. B., Frank, A. B., Haferkamp, M. R., Meyers,
583 T. P., and Morgan, J. A.: Integration of CO₂ flux and remotely-sensed data for primary production and
584 ecosystem respiration analyses in the Northern Great Plains: potential for quantitative spatial
585 extrapolation, *Global Ecology and Biogeography*, 14, 271-292, 10.1111/j.1466-822X.2005.00151.x, 2005.

586 Gornall, J. L., Jonsdottir, I. S., Woodin, S. J., and Van der Wal, R.: Arctic mosses govern below-ground
587 environment and ecosystem processes, *Oecologia*, 153, 931-941, 10.1007/s00442-007-0785-0, 2007.

588 Gornall, J. L., Woodin, S. J., Jonsdottir, I. S., and van der Wal, R.: Balancing positive and negative plant
589 interactions: how mosses structure vascular plant communities, *Oecologia*, 166, 769-782,
590 10.1007/s00442-011-1911-6, 2011.

591 Gough, C. M., Hardiman, B. S., Nave, L. E., Bohrer, G., Maurer, K. D., Vogel, C. S., Nadelhoffer, K. J.,
592 and Curtis, P. S.: Sustained carbon uptake and storage following moderate disturbance in a Great Lakes
593 forest, *Ecological Applications*, 23, 1202-1215, 2013.

594 Goulden, M. L., Winston, G. C., McMillan, A. M. S., Litvak, M. E., Read, E. L., Rocha, A. V., and Rob
595 Elliot, J.: An eddy covariance mesonet to measure the effect of forest age on land atmosphere exchange,
596 *Global change biology*, 12, 2146-2162, 10.1111/j.1365-2486.2006.01251.x, 2006.

597 Hansen, J., Sato, M., Ruedy, R., Lo, K., Lea, D. W., and Medina-Elizade, M.: Global temperature change,
598 Proceedings of the National Academy of Sciences of the United States of America, 103, 14288-14293,
599 10.1073/pnas.0606291103, 2006.

600 Harris, I., Jones, P. D., Osborn, T. J., and Lister, D. H.: Updated high-resolution grids of monthly climatic
601 observations - the CRU TS3.10 Dataset, International Journal of Climatology, 34, 623-642,
602 10.1002/joc.3711, 2014.

603 Hayes, D. J., McGuire, A. D., Kicklighter, D. W., Gurney, K. R., Burnside, T. J., and Melillo, J. M.: Is the
604 northern high-latitude land-based CO₂ sink weakening?, Global Biogeochemical Cycles, 25, n/a-n/a,
605 10.1029/2010gb003813, 2011.

606 Hayes, D. J., Kicklighter, D. W., McGuire, A. D., Chen, M., Zhuang, Q., Yuan, F., Melillo, J. M., and
607 Wullschleger, S. D.: The impacts of recent permafrost thaw on land-atmosphere greenhouse gas
608 exchange, Environmental Research Letters, 9, 045005, 10.1088/1748-9326/9/4/045005, 2014.

609 Xiaolan He, Kate S. He, Jaakko Hyvönen, Will bryophytes survive in a warming world?,
610 Perspectives in Plant Ecology, Evolution and Systematics, Volume 19, 2016, Pages 49-60,
611 ISSN 1433-8319, <https://doi.org/10.1016/j.ppees.2016.02.005>.

612 Hiller, R. V., McFadden, J. P., and Kljun, N.: Interpreting CO₂ Fluxes Over a Suburban Lawn: The
613 Influence of Traffic Emissions, Boundary-Layer Meteorology, 138, 215-230, 10.1007/s10546-010-9558-
614 0, 2010.

615 Hugelius, G., Strauss, J., Zubrzycki, S., Harden, J. W., Schuur, E. A. G., Ping, C. L., Schirmer, L.,
616 Grosse, G., Michaelson, G. J., Koven, C. D., amp, apos, Donnell, J. A., Elberling, B., Mishra, U., Camill,
617 P., Yu, Z., Palmtag, J., and Kuhry, P.: Estimated stocks of circumpolar permafrost carbon with quantified
618 uncertainty ranges and identified data gaps, Biogeosciences, 11, 6573-6593, 10.5194/bg-11-6573-2014,
619 2014.

620 Jägerbrand, A. K., Lindblad, K. E. M., Björk, R. G., Alatalo, J. M., and Molau, U.: Bryophyte and Lichen
621 Diversity Under Simulated Environmental Change Compared with Observed Variation in Unmanipulated
622 Alpine Tundra, Biodiversity and Conservation, 15, 4453-4475, 10.1007/s10531-005-5098-1, 2006.

623 Jenkins, J. P., Richardson, A. D., Braswell, B. H., Ollinger, S. V., Hollinger, D. Y., and Smith, M. L.:
624 Refining light-use efficiency calculations for a deciduous forest canopy using simultaneous tower-based
625 carbon flux and radiometric measurements, Agricultural and Forest Meteorology, 143, 64-79,
626 10.1016/j.agrformet.2006.11.008, 2007.

627 Juha M Alatalo, Annika K Jägerbrand, Mohammad Bagher Erfanian, Shengbin Chen, Shou-Qin Sun, Ulf
628 Molau, Bryophyte cover and richness decline after 18 years of experimental warming in alpine Sweden,
629 AoB PLANTS, Volume 12, Issue 6, December 2020, plaa061, <https://doi.org/10.1093/aobpla/plaa061>

630 Kasischke, E. S.: Boreal ecosystems in the global carbon cycle. In Fire, climate change, and carbon
631 cycling in the boreal forest, *Ecological Studies (Analysis and Synthesis)*, 138, 19-30,
632 https://doi.org/10.1007/978-0-387-21629-4_2, 2000.

633 Kasischke, E. S., and Turetsky, M. R.: Recent changes in the fire regime across the North American
634 boreal region—Spatial and temporal patterns of burning across Canada and Alaska, *Geophysical Research*
635 *Letters*, 33, 10.1029/2006gl025677, 2006.

636 Kip, N., Ouyang, W., van Winden, J., Raghoebarsing, A., van Niftrik, L., Pol, A., Pan, Y., Bodrossy, L.,
637 van Donselaar, E. G., Reichart, G. J., Jetten, M. S., Damste, J. S., and Op den Camp, H. J.: Detection,
638 isolation, and characterization of acidophilic methanotrophs from Sphagnum mosses, *Applied and*
639 *environmental microbiology*, 77, 5643-5654, 10.1128/AEM.05017-11, 2011.

640 Knorr, W.: Annual and interannual CO₂ exchanges of the terrestrial biosphere: process-based simulations
641 and uncertainties, *Global Ecology and Biogeography*, 9, 225-252, 2000.

642 Koven, C. D., Schuur, E. A. G., Schädel, C., Bohn, T. J., Burke, E. J., Chen, G., Chen, X., Ciais, P.,
643 Grosse, G., Harden, J. W., Hayes, D. J., Hugelius, G., Jafarov, E. E., Krinner, G., Kuhry, P., Lawrence, D.
644 M., Macdougall, A. H., Marchenko, S. S., Mcguire, A. D., Natali, S. M., Nicolsky, D. J., Olefeldt, D.,
645 Peng, S., Romanovsky, V. E., Schaefer, K. M., Strauss, J., Treat, C. C. & Turetsky, M. 2015. A simplified,
646 data-constrained approach to estimate the permafrost carbon-climate feedback. *Philosophical*
647 *Transactions of the Royal Society A: Mathematical, Physical and Engineering Sciences*, 373.

648 L. Kulmala, J. P., P. Hari and T. Vesala: Photosynthesis of ground vegetation in different aged pine forests:
649 Effect of environmental factors predicted with a process-based model, *Journal of Vegetation Science*, 22,
650 96–110, 2011.

651 Launiainen, S., Katul, G. G., Lauren, A., and Kolari, P.: Coupling boreal forest CO₂, H₂O and energy
652 flows by a vertically structured forest canopy – Soil model with separate bryophyte layer, *Ecological*
653 *Modelling*, 312, 385-405, 10.1016/j.ecolmodel.2015.06.007, 2015.

654 Lindo, Z., and Gonzalez, A.: The Bryosphere: An Integral and Influential Component of the Earth's
655 Biosphere, *Ecosystems*, 13, 612-627, 10.1007/s10021-010-9336-3, 2010.

656 Lang, S.I., Cornelissen, J.H.C., Shaver, G.R., Ahrens, M., Callaghan, T.V., Molau, U., Ter Braak, C.J.F.,
657 Hölzer, A. and Aerts, R. (2012), Arctic warming on two continents has consistent negative effects on
658 lichen diversity and mixed effects on bryophyte diversity. *Glob Change Biol*, 18: 1096-1107.
659 <https://doi.org/10.1111/j.1365-2486.2011.02570.x>

660 Longton, R. E.: Adaptations and strategies of polar bryophytes, *Botanical Journal of the Linnean Society*,
661 98, 253-268, 1988.

662 Markham, J. H.: Variation in moss-associated nitrogen fixation in boreal forest stands, *Oecologia*, 161,
663 353-359, 10.1007/s00442-009-1391-0, 2009.

664 McEwing, K. R., Fisher, J. P., and Zona, D.: Environmental and vegetation controls on the spatial
665 variability of CH₄ emission from wet-sedge and tussock tundra ecosystems in the Arctic, *Plant and soil*,
666 388, 37-52, 10.1007/s11104-014-2377-1, 2015.

667 McGuire, A. D., Melillo, J. M., Joyce, L. A., Kicklighter, D. W., Grace, A. L., III, B. M., and Vorosmarty,
668 C. J.: Interactions between carbon and nitrogen dynamics in estimating net primary productivity for
669 potential vegetation in North America, *Global Biogeochemical Cycles*, 6, 101-124, 1992.

670 McGuire, A. D., Melillo, J. M., Kicklighter, D. W., and Joyce, L. A.: Equilibrium responses of soil carbon
671 to climate change: Empirical and process-based estimates, *Journal of Biogeography*, 785-796, 1995.

672 McGuire, A. D., and Hobbie, J. E.: Global climate change and the equilibrium responses of carbon
673 storage in arctic and subarctic regions, In *Modeling the Arctic system: A workshop report on the state of*
674 *modeling in the Arctic System Science program*, 53-54, 1997.

675 McGuire, A. D., Anderson, L. G., Christensen, T. R., Dallimore, S., Guo, L., Hayes, D. J., Heimann, M.,
676 Lorenson, T. D., Macdonald, R. W., and Roulet, N.: Sensitivity of the carbon cycle in the Arctic to climate
677 change, *Ecological Monographs*, 79, 523-555, 2009.

678 Melillo, J. M., McGuire, A. D., Kicklighter, D. W., Moore, B., Vorosmarty, C. J., and Schloss, A. L.:
679 Global climate change and terrestrial net primary production, *Nature*, 363, 234, 10.1038/363234a0, 1993.

680 Melillo, J. M., Butler, S., Johnson, J., Mohan, J., Steudler, P., Lux, H., Burrows, E., Bowles, F., Smith, R.,
681 Scott, L., Vario, C., Hill, T., Burton, A., Zhou, Y.-M., and Tang, J.: Soil warming, carbon - nitrogen
682 interactions, and forest carbon budgets, *PNAS*, 108, 9508-9512, 2011.

683 Naomi Oreskes, K. S.-F., Kenneth Belitz: Verification, validation, and confirmation of numerical models
684 in the earth sciences, *Science*, 263, 641-646, 1994.

685 O. Skre, W. C. O.: Moss production in a black spruce *Picea mariana* forest with permafrost near
686 Fairbanks, Alaska, as compared with two permafrost-free stands, *Ecography*, 2, 249-254, 1979.

687 Oechel, W. C., Laskowski, C. A., Burba, G., Gioli, B., and Kalhori, A. A. M.: Annual patterns and budget
688 of CO₂ flux in an Arctic tussock tundra ecosystem, *Journal of Geophysical Research: Biogeosciences*,
689 119, 323-339, 10.1002/2013jg002431, 2014.

690 Okland, R. H.: Population Biology of the Clonal Moss *Hylocomium Splendens* in Norwegian Boreal
691 Spruce Forests. I. Demography, *Journal of Ecology*, 83, 697-712, 1995.

692 P.C. Harley, J. D. T., K.J. Murray, and J. Beyers: Irradiance and temperature effects on photosynthesis of
693 tussock tundra *Sphagnum* mosses from the foothills of the Philip Smith Mountains, Alaska, *Oecologia*,
694 79, 251-259, 1989.

695 Pakarinen, P., and D. H. Vitt: Primary production of plant communities of the Truelove Lowland, Devon
696 Island, Canada—Moss communities, Primary production and production processes, tundra biome.
697 International Biological Programme, Tundra Biome Steering Committee, Edmonton Oslo, 37-46, 1973.

698 Pharo, E. J., and Zartman, C. E.: Bryophytes in a changing landscape: The hierarchical effects of habitat
699 fragmentation on ecological and evolutionary processes, *Biological Conservation*, 135, 315-325,
700 10.1016/j.biocon.2006.10.016, 2007.

701 Raich, J. W., Rastetter, E. B., Melillo, J. M., Kicklighter, D. W., Steudler, P. A., Peterson, B. J., Grace, A.
702 L., III, B. M., and Vorosmarty, C. J.: Potential net primary productivity in South America: application of a
703 global model, *Ecological Applications*, 1, 399-429, 1991.

704 Richardson, A. D., Jenkins, J. P., Braswell, B. H., Hollinger, D. Y., Ollinger, S. V., and Smith, M. L.: Use
705 of digital webcam images to track spring green-up in a deciduous broadleaf forest, *Oecologia*, 152, 323-
706 334, 10.1007/s00442-006-0657-z, 2007.

707 Running, S. W., and Coughlan, J. C.: A general model of forest ecosystem processes for regional
708 applications I. Hydrologic balance, canopy gas exchange and primary production processes., *Ecological*
709 *Modelling*, 42, 125-154, 1988.

710 S. Frohking, M. L. G., S.C. Wofsy, S-M. Fan, D.J. Sutton, J.W. Munger, A.M. Bazzaz, B.C. Daube, P.M.
711 Crill, J.D, Aber, L.E. Band, X. Wang, K. Savage, T. Moore and R.C. Harriss: Modelling temporal
712 variability in the carbon balance of a spruce/moss boreal forest, *Global change biology*, 2, 343-366, 1996.

713 Sarah E. Hobbie, J. P. S., Susan E. Trumbore and James R. Randerson: Controls over carbon storage and
714 turnover in high-latitude soils, *Global change biology*, 6, 196-210, 2000.

715 Schimel, D. S., House, J. I., Hibbard, K. A., Bousquet, P., Ciais, P., Peylin, P., Braswell, B. H., Apps, M.
716 J., Baker, D., Bondeau, A., Canadell, J., Churkina, G., Cramer, W., Denning, A. S., Field, C. B.,
717 Friedlingstein, P., Goodale, C., Heimann, M., Houghton, R. A., Melillo, J. M., III, B. M., Murdiyarso, D.,
718 Noble, I., Pacala, S. W., Prentice, I. C., Raupach, M. R., Rayner, P. J., Scholes, R. J., Steffen, W. L., and
719 Wirth, C.: Recent patterns and mechanisms of carbon exchange by terrestrial ecosystems, *Nature*, 414,
720 2001.

721 Serreze, M. C., and Francis, J. A.: The Arctic on the fast track of change, *Weather*, 61, 65-69, 2006.

722 Shetler, G., Turetsky, M. R., Kane, E., and Kasischke, E.: Sphagnum mosses limit total carbon
723 consumption during fire in Alaskan black spruce forests, *Canadian Journal of Forest Research*, 38, 2328-
724 2336, 10.1139/x08-057, 2008.

725 Soja, A. J., Tchepakova, N. M., French, N. H. F., Flannigan, M. D., Shugart, H. H., Stocks, B. J.,
726 Sukhinin, A. I., Parfenova, E. I., Chapin, F. S., and Stackhouse, P. W.: Climate-induced boreal forest
727 change: Predictions versus current observations, *Global and Planetary Change*, 56, 274-296,
728 10.1016/j.gloplacha.2006.07.028, 2007.

729 Stow, D. A., Hope, A., McGuire, D., Verbyla, D., Gamon, J., Huemmrich, F., Houston, S., Racine, C.,
730 Sturm, M., Tape, K., Hinzman, L., Yoshikawa, K., Tweedie, C., Noyle, B., Silapaswan, C., Douglas, D.,
731 Griffith, B., Jia, G., Epstein, H., Walker, D., Daeschner, S., Petersen, A., Zhou, L., and Myneni, R.:

732 Remote sensing of vegetation and land-cover change in Arctic Tundra Ecosystems, *Remote Sensing of*
733 *Environment*, 89, 281-308, 10.1016/j.rse.2003.10.018, 2004.

734 T. G. Williams, L. B. F.: Measuring and modelling environmental influences on photosynthetic gas
735 exchange in Sphagnum and Pleurozium, *Plant, Cell and Environment*, 21, 555–564, 1998.

736 Tang, J., and Zhuang, Q.: Equifinality in parameterization of process-based biogeochemistry models: A
737 significant uncertainty source to the estimation of regional carbon dynamics, *Journal of Geophysical*
738 *Research: Biogeosciences*, 113, 10.1029/2008jg000757, 2008.

739 Tape, K. E. N., Sturm, M., and Racine, C.: The evidence for shrub expansion in Northern Alaska and the
740 Pan-Arctic, *Global change biology*, 12, 686-702, 10.1111/j.1365-2486.2006.01128.x, 2006.

741 Tarnocai, C., Canadell, J. G., Schuur, E. A. G., Kuhry, P., Mazhitova, G., and Zimov, S.: Soil organic
742 carbon pools in the northern circumpolar permafrost region, *Global Biogeochemical Cycles*, 23, n/a-n/a,
743 10.1029/2008gb003327, 2009.

744 Todd-Brown, K. E. O., Randerson, J. T., Post, W. M., Hoffman, F. M., Tarnocai, C., Schuur, E. A. G., and
745 Allison, S. D.: Causes of variation in soil carbon simulations from CMIP5 Earth system models and
746 comparison with observations, *Biogeosciences*, 10, 1717-1736, 10.5194/bg-10-1717-2013, 2013.

747 Treseder, K. K., Balser, T. C., Bradford, M. A., Brodie, E. L., Dubinsky, E. A., Eviner, V. T., Hofmockel,
748 K. S., Lennon, J. T., Levine, U. Y., MacGregor, B. J., Pett-Ridge, J., and Waldrop, M. P.: Integrating
749 microbial ecology into ecosystem models: challenges and priorities, *Biogeochemistry*, 109, 7-18,
750 10.1007/s10533-011-9636-5, 2011.

751 Treseder, K. K., Marusenko, Y., Romero-Olivares, A. L., and Maltz, M. R.: Experimental warming alters
752 potential function of the fungal community in boreal forest, *Global change biology*, 22, 3395-3404,
753 10.1111/gcb.13238, 2016.

754 Turetsky, M. R., Mack, M. C., Hollingsworth, T. N., and Harden, J. W.: The role of mosses in ecosystem
755 succession and function in Alaska's boreal forest This article is one of a selection of papers from The
756 *Dynamics of Change in Alaska's Boreal Forests: Resilience and Vulnerability in Response to Climate*
757 *Warming*, *Canadian Journal of Forest Research*, 40, 1237-1264, 10.1139/x10-072, 2010.

758 Turetsky, M. R., Bond-Lamberty, B., Euskirchen, E., Talbot, J., Frohking, S., McGuire, A. D., and Tuittila,
759 E. S.: The resilience and functional role of moss in boreal and arctic ecosystems, *The New phytologist*,
760 196, 49-67, 10.1111/j.1469-8137.2012.04254.x, 2012.

761 Wardle, M.-C. N. a. D. A.: Understory vegetation as a forest ecosystem driver: evidence from the northern
762 Swedish boreal forest, *The Ecological Society of America*, 3, 421–428, 2005.

763 White, A., Cannell, M. G. R., and Friend, A. D.: The high-latitude terrestrial carbon sink: a model analysis
764 *Global change biology*, 6, 227-245, 2000.

765 Wieder, W. R., Bonan, G. B., and Allison, S. D.: Global soil carbon projections are improved by
766 modelling microbial processes, *Nature Climate Change*, 3, 909-912, 10.1038/nclimate1951, 2013.

767 Zha, J., and Zhuang, Q.: Microbial decomposition processes and vulnerable Arctic soil organic carbon in
768 the 21st century, *Biogeosciences Discussions*, 1-34, 10.5194/bg-2018-241, 2018.

769 Zhuang, Q., Romanovsky, V. E., and McGuire, A. D.: Incorporation of a permafrost model into a large-
770 scale ecosystem model: Evaluation of temporal and spatial scaling issues in simulating soil thermal
771 dynamics, *Journal of Geophysical Research: Atmospheres*, 106, 33649-33670, 10.1029/2001jd900151,
772 2001.

773 Zhuang, Q., McGuire, A. D., O'Neill, K. P., Harden, J. W., Romanovsky, V. E., and Yarie, J.: Modeling
774 soil thermal and carbon dynamics of a fire chronosequence in interior Alaska, *Journal of Geophysical
775 Research*, 108, 10.1029/2001jd001244, 2002.

776 Zhuang, Q., A. D. McGuire, J. M. Melillo, J. S. Clein, R. J. Dargaville, D. W. Kicklighter, R. B. Myneni,
777 J. Dong, V. E. Romanovsky, J. Harden, J. E. Hobbie (2003) Carbon cycling in extratropical terrestrial
778 ecosystems of the Northern Hemisphere during the 20th Century: A modeling analysis of the influences of
779 soil thermal dynamics, *Tellus*, 55B, 751-776, 2003

780 Zhuang, Q., He, J., Lu, Y., Ji, L., Xiao, J., and Luo, T.: Carbon dynamics of terrestrial ecosystems on the
781 Tibetan Plateau during the 20th century: an analysis with a process-based biogeochemical model, *Global
782 Ecology and Biogeography*, 19, 649-662, 10.1111/j.1466-8238.2010.00559.x, 2010.

783 Zhuang, Q., Chen, M., Xu, K., Tang, J., Saikawa, E., Lu, Y., Melillo, J. M., Prinn, R. G., and McGuire, A.
784 D.: Response of global soil consumption of atmospheric methane to changes in atmospheric climate and
785 nitrogen deposition, *Global Biogeochemical Cycles*, 27, 650-663, 10.1002/gbc.20057, 2013.

786 Zhuang, Q., Zhu, X., He, Y., Prigent, C., Melillo, J. M., David McGuire, A., Prinn, R. G., and Kicklighter,
787 D. W.: Influence of changes in wetland inundation extent on net fluxes of carbon dioxide and methane in
788 northern high latitudes from 1993 to 2004, *Environmental Research Letters*, 10, 095009, 10.1088/1748-
789 9326/10/9/095009, 2015.

790

791

792

793

794 **Author contributions.** Q.Z. designed the study. J.Z. conducted model development, simulation
795 and analysis. J.Z. and Q. Z. wrote the paper.

796 **Competing financial interests.** The submission has no competing financial interests.

797 **Materials & Correspondence.** Correspondence and material requests should be addressed to

798 qzhuang@purdue.edu.

799

800

801

802

803

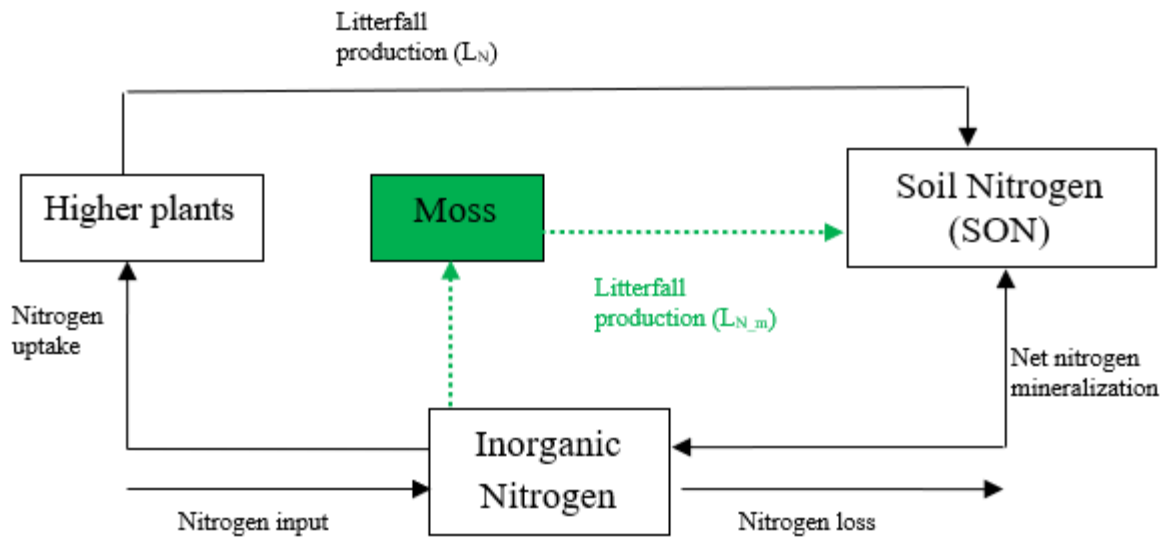
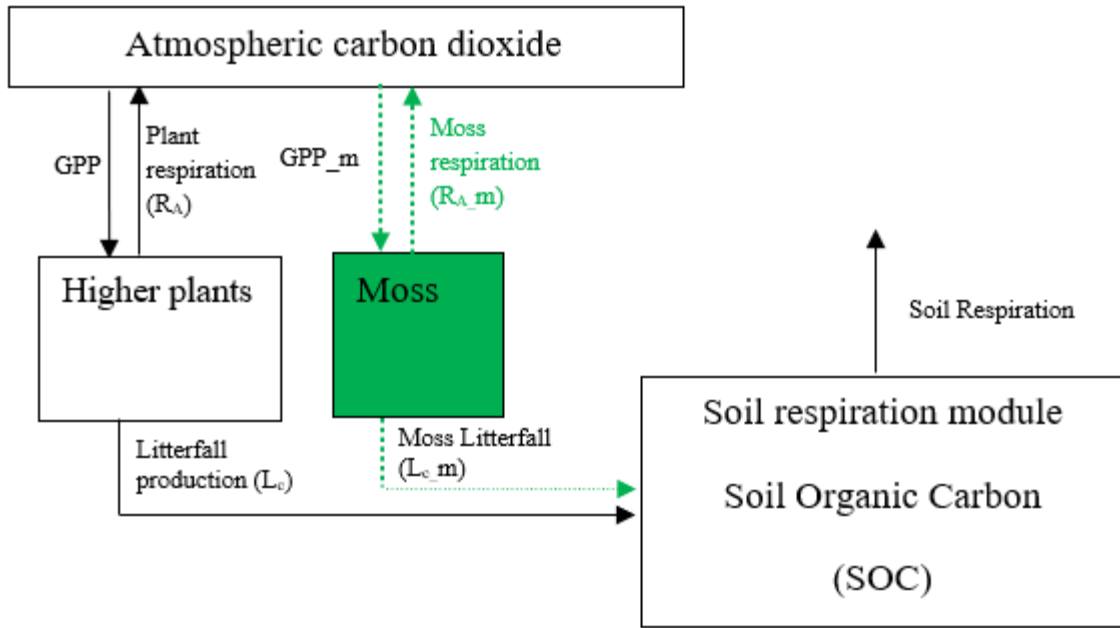
804

805

806

807

808

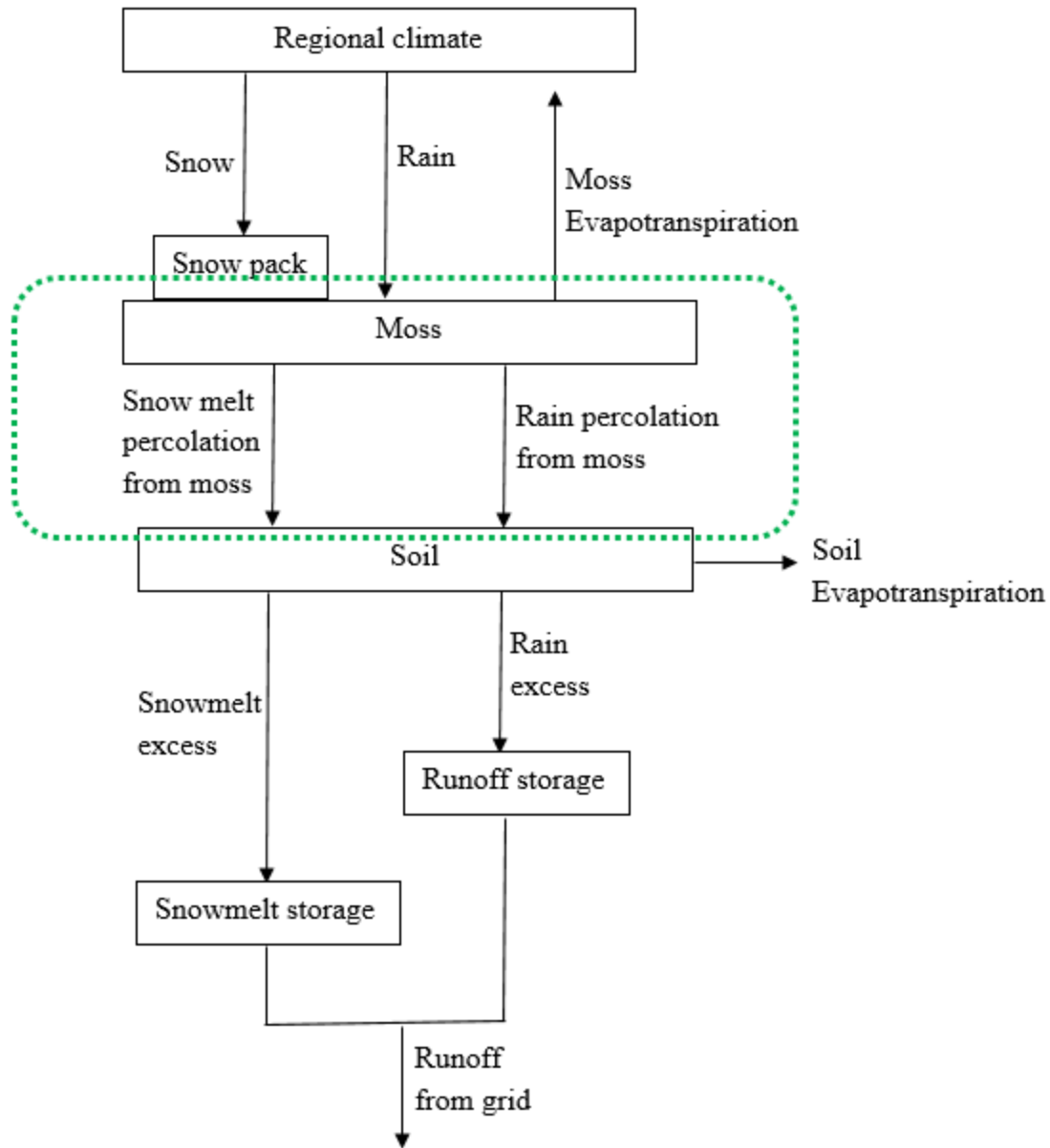


809

810 Figure 1. Schematic diagram of TEM_Moss: Green dashed arrows are new carbon and nitrogen
 811 fluxes, representing moss production, moss respiration and litterfall of moss. Black arrows were
 812 in TEM 5.0 (Zhuang et al., 2013).

813

814



815

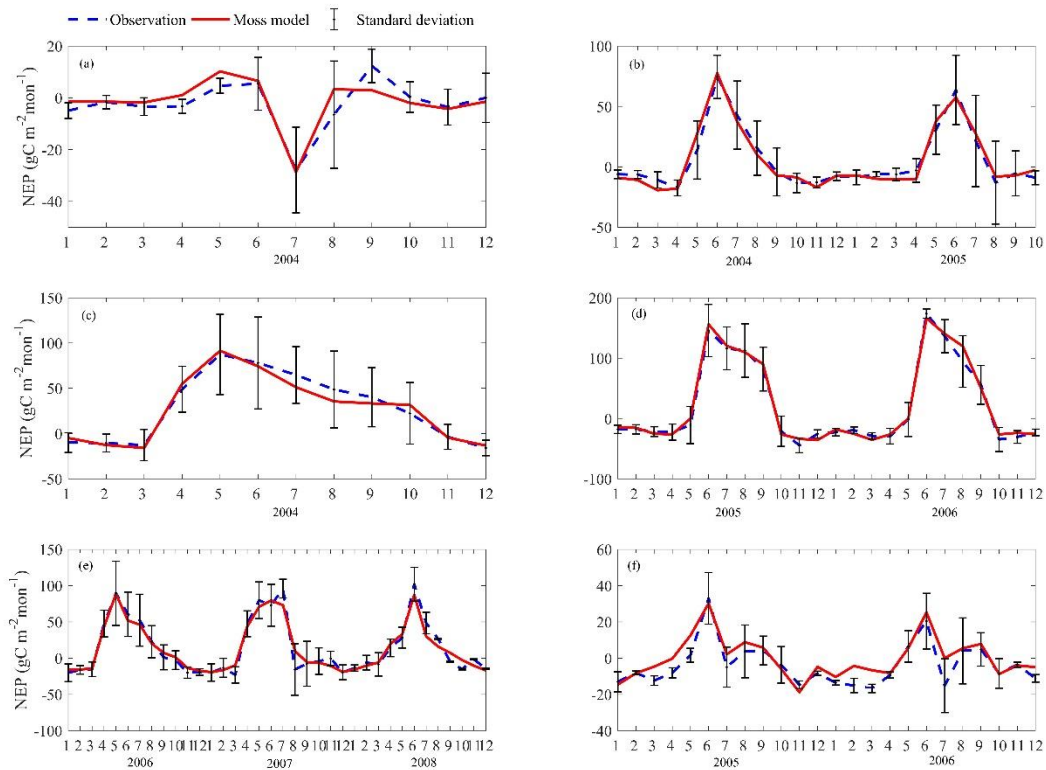
816 Figure 2. The revised Water Balance Model: Green dashed circle represents the hydrology
 817 dynamics for moss (Vörösmarty et al., 1989).

818

819

820

821



822

823 Figure 3. Comparison between observed and simulated NEP ($\text{gC m}^{-2}\text{mon}^{-1}$) at: (a) Ivotuk (alpine
 824 tundra), (b) UCI-1964 burn site (boreal forest), (c) Howland Forest (main tower) (temperate
 825 coniferous forest), (d) Univ. of Mich. Biological Station (Temperate deciduous forest), (e)
 826 KUOM Turfgrass Field (Grassland), and (f) Atqasuk (Wet tundra). Note: scales are different.
 827 Error bars represent standard errors among daily measure data in one month.

828

829

830

831

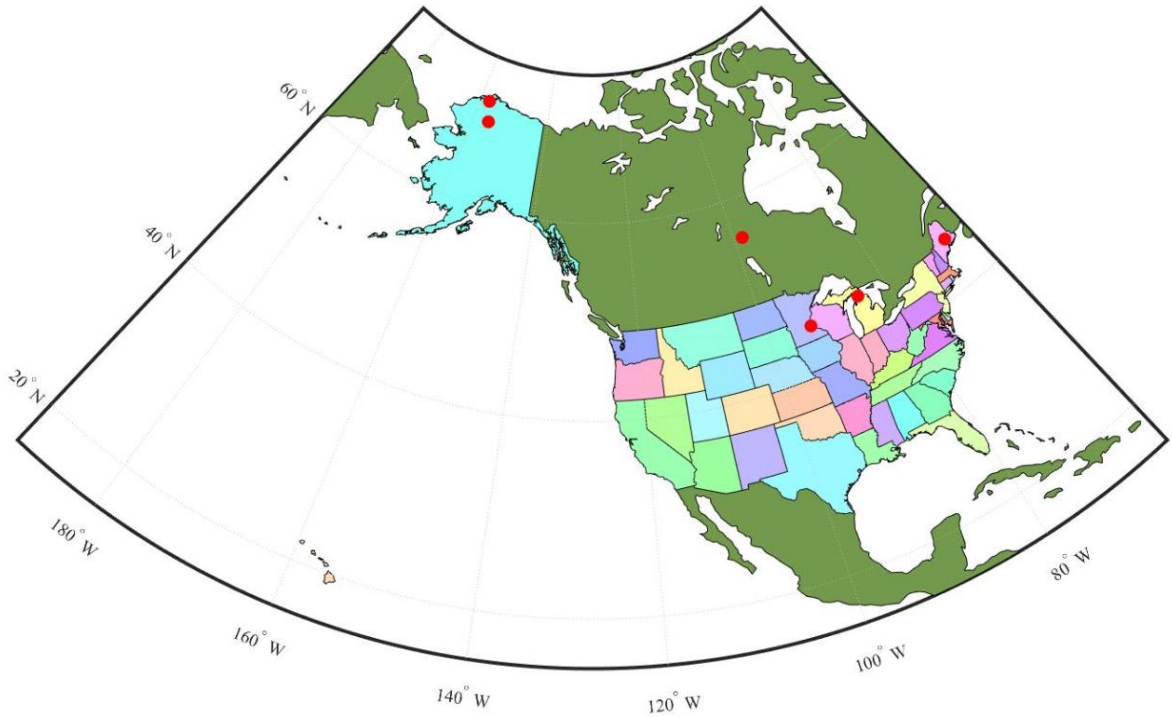
832

833

834

835

836



837

838 Figure 4. Map showing six sites used for TEM_Moss calibration. The red points represent the six
 839 sites, **five** which are **all** in **the** US **and one is in the Canada**: US-Ivo: Ivotuk (alpine tundra), CA-
 840 NS3: UCI-1964 burn site (boreal forest), US-Ho1: Howland Forest (temperate coniferous forest),
 841 US-UMB: Univ. of Mich. Biological Station (temperate deciduous forest), US-KUT: KUOM
 842 Turfgrass Field (grassland), US-Atq: Atqasuk (wet tundra).

843

844

845

846

847

848

849

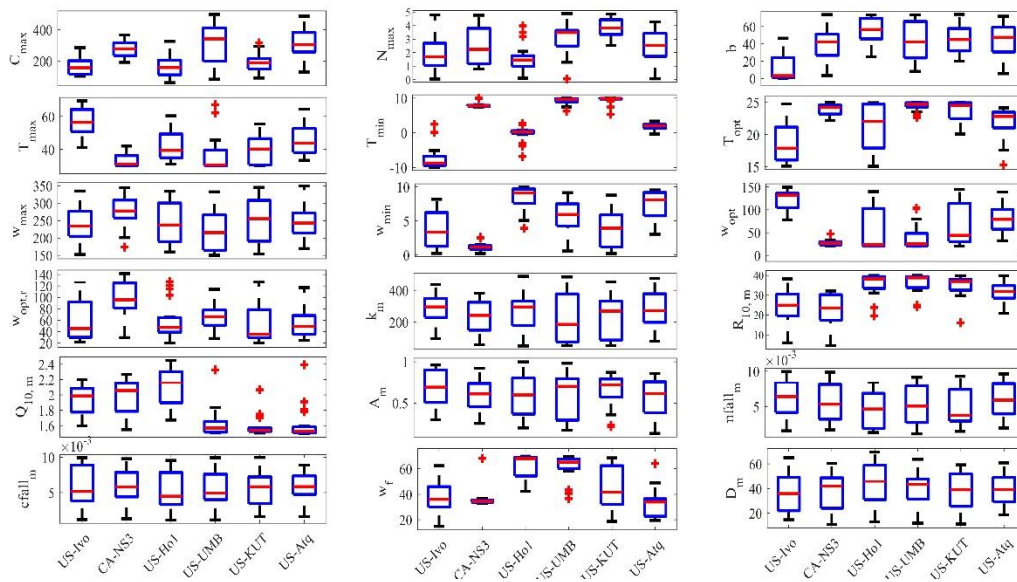
850

851

852

853

854



855

856 Figure 5. Boxplot of parameter posterior distribution that are obtained after ensemble inverse
 857 modeling for TEM_Moss at all six sites: US-Ivo: Ivotuk (alpine tundra), CA-NS3: UCI-1964
 858 burn site (boreal forest), US-Hol: Howland Forest (temperate coniferous forest), US-UMB:
 859 Univ. of Mich. Biological Station (temperate deciduous forest), US-KUT: KUOM Turfgrass
 860 Field (grassland), US-Atq: Atqasuk (wet tundra). Boxes represent the range between the first
 861 quartile and the third quartile of the parameter values, the red line within box represents the
 862 second quartile or the mean of the values. The bottom and top whiskers represent minimum and
 863 maximum parameter values, respectively.

864

865

866

867

868

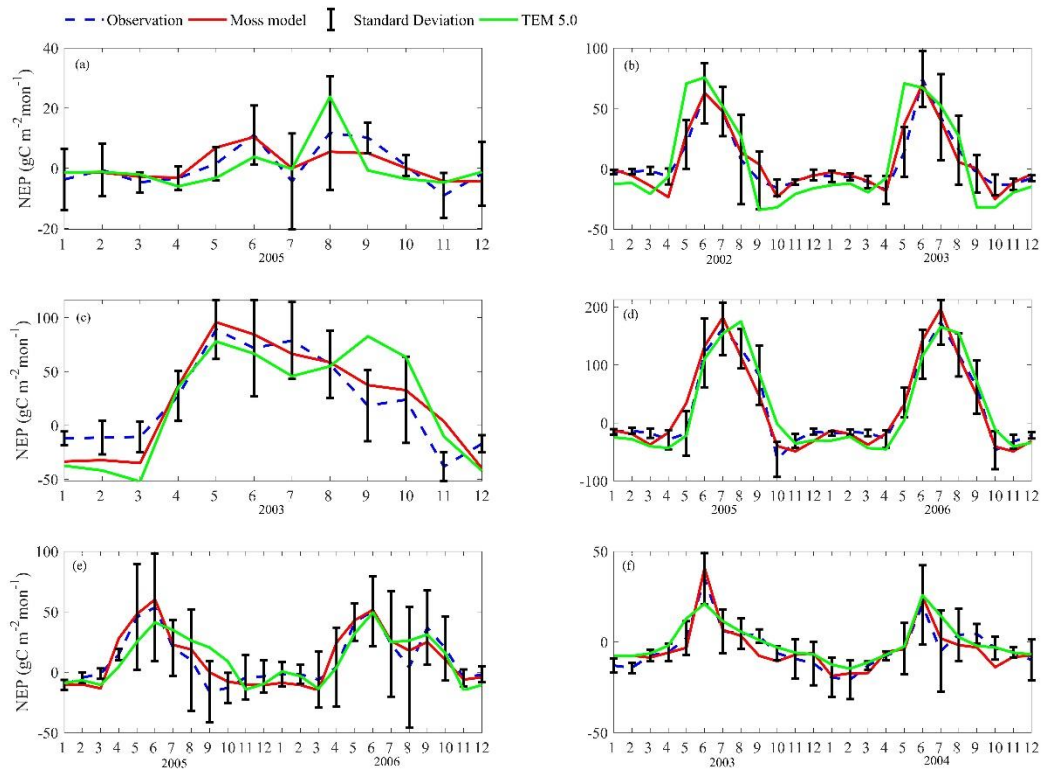
869

870

871

872

873



874

875 Figure 6. Comparison between observed and simulated NEP ($\text{gC m}^{-2}\text{mon}^{-1}$) at: (a) Ivotuk (alpine
 876 tundra), (b) UCI-1964 burn site (boreal forest), (c) Howland Forest (main tower) (temperate
 877 coniferous forest), (d) Bartlett Experimental Forest (Temperate deciduous forest), (e) Brookings
 878 (Grassland), and (f) Atqasuk (Wet tundra). Note: scales are different.

879

880

881

882

883

884

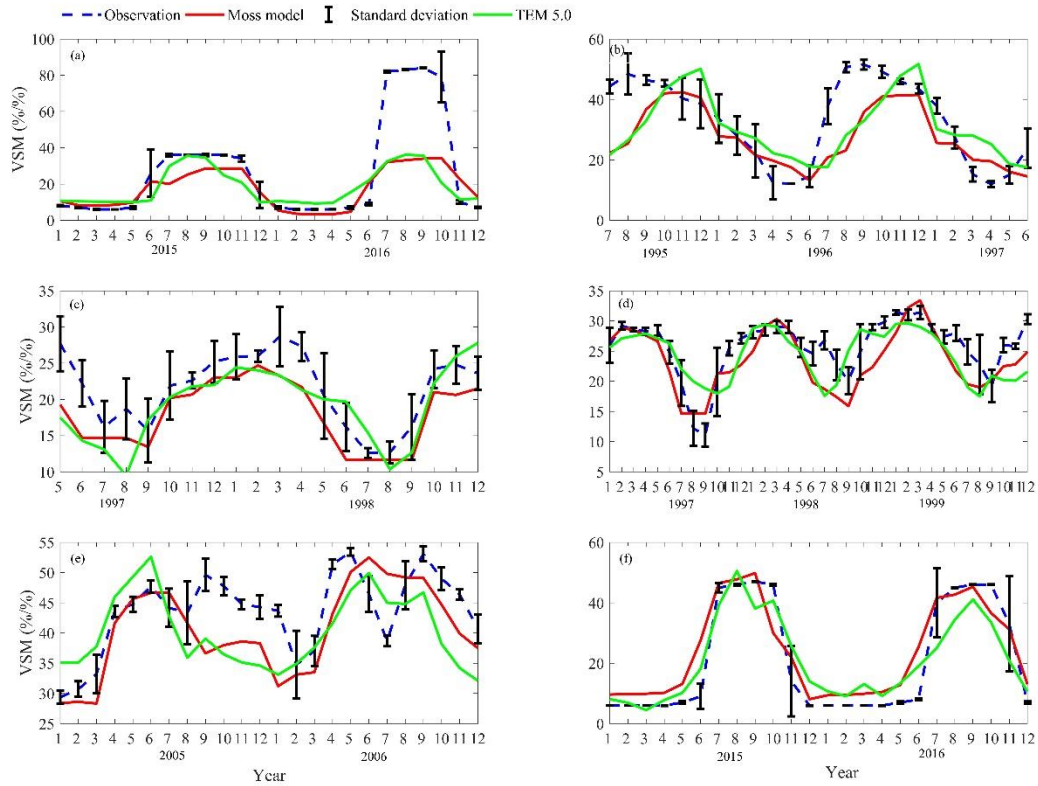
885

886

887

888

889



890

891 Figure 7. Comparison between observed and simulated volumetric soil moisture (VSM, %/%) at:
 892 (a) US-Ivo (alpine tundra), (b) BOREAS NSA-OBS (boreal forest), (c) NL-Loo (temperate
 893 coniferous forest), (d) DK-Sor (Temperate deciduous forest), (e) US-Bkg (Grassland), and (f)
 894 US-Atq (Wet tundra). Note: scales are different.

895

896

897

898

899

900

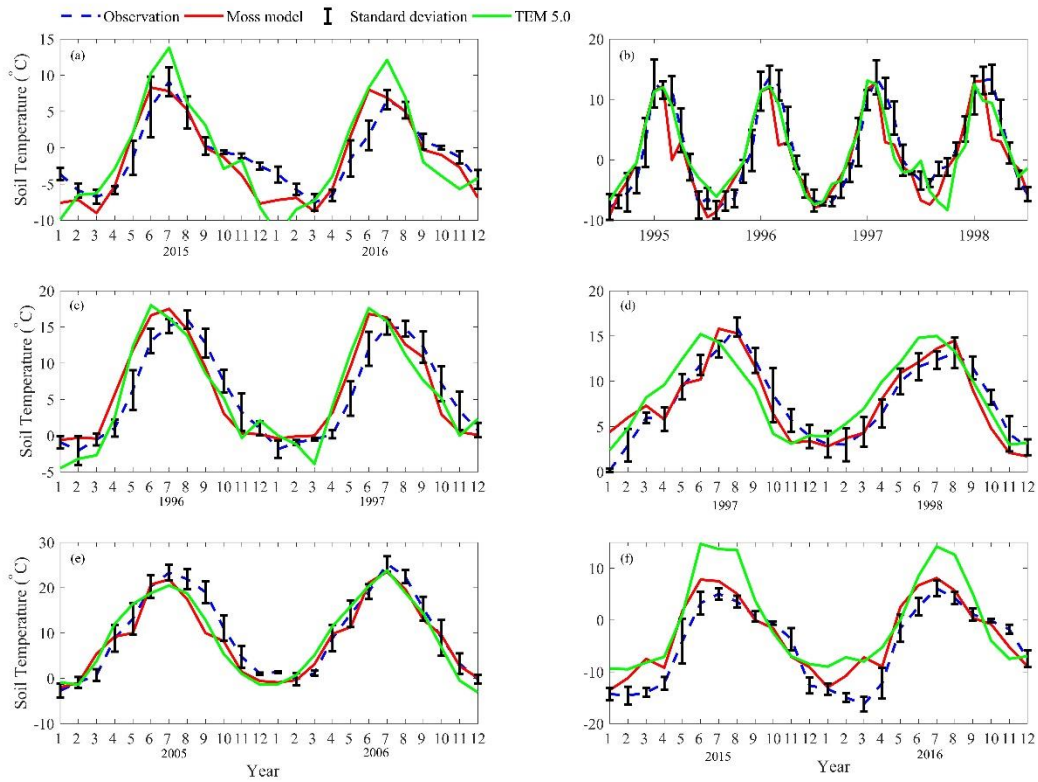
901

902

903

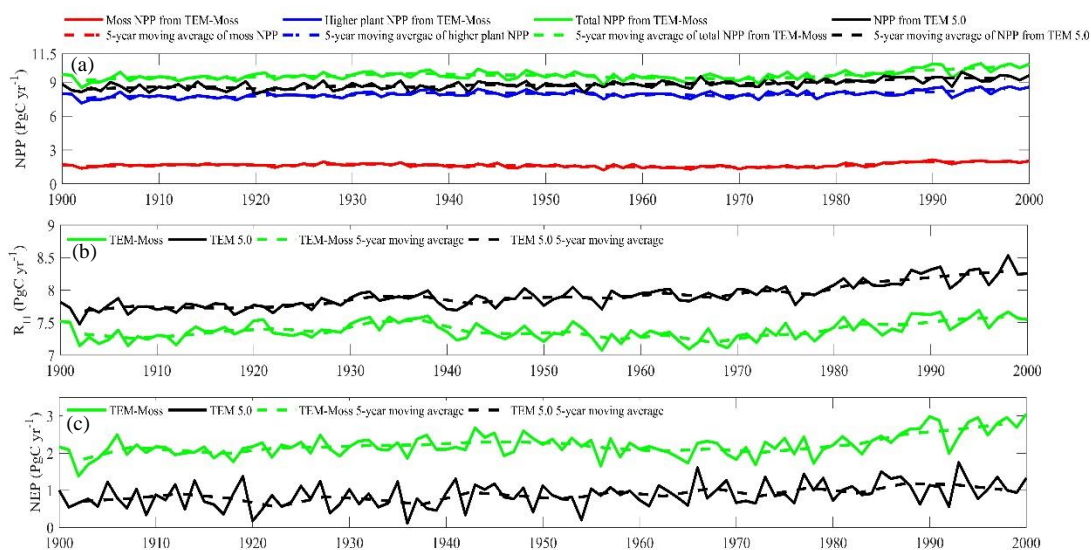
904

905



906
 907 Figure 8. Comparison between observed and simulated soil temperature at 5cm depth (°C) at: (a)
 908 US-Ivo (alpine tundra), (b) BOREAS NSA-OBS (boreal forest), (c) US-Ho1 (temperate
 909 coniferous forest), (d) BE-Vie (Temperate deciduous forest), (e) US-Bkg (Grassland), and (f)
 910 US-Atq (Wet tundra). Note: scales are different.

911
 912
 913
 914
 915
 916
 917
 918
 919
 920
 921
 922



923

924 Figure 9. Simulated annual net primary production (NPP, a), heterotrophic respiration (R_H , b),
 925 and net ecosystem production (NEP, c) during the 20th century by TEM_Moss and TEM 5.0.

926

927

928

929

930

931

932

933

934

935

936

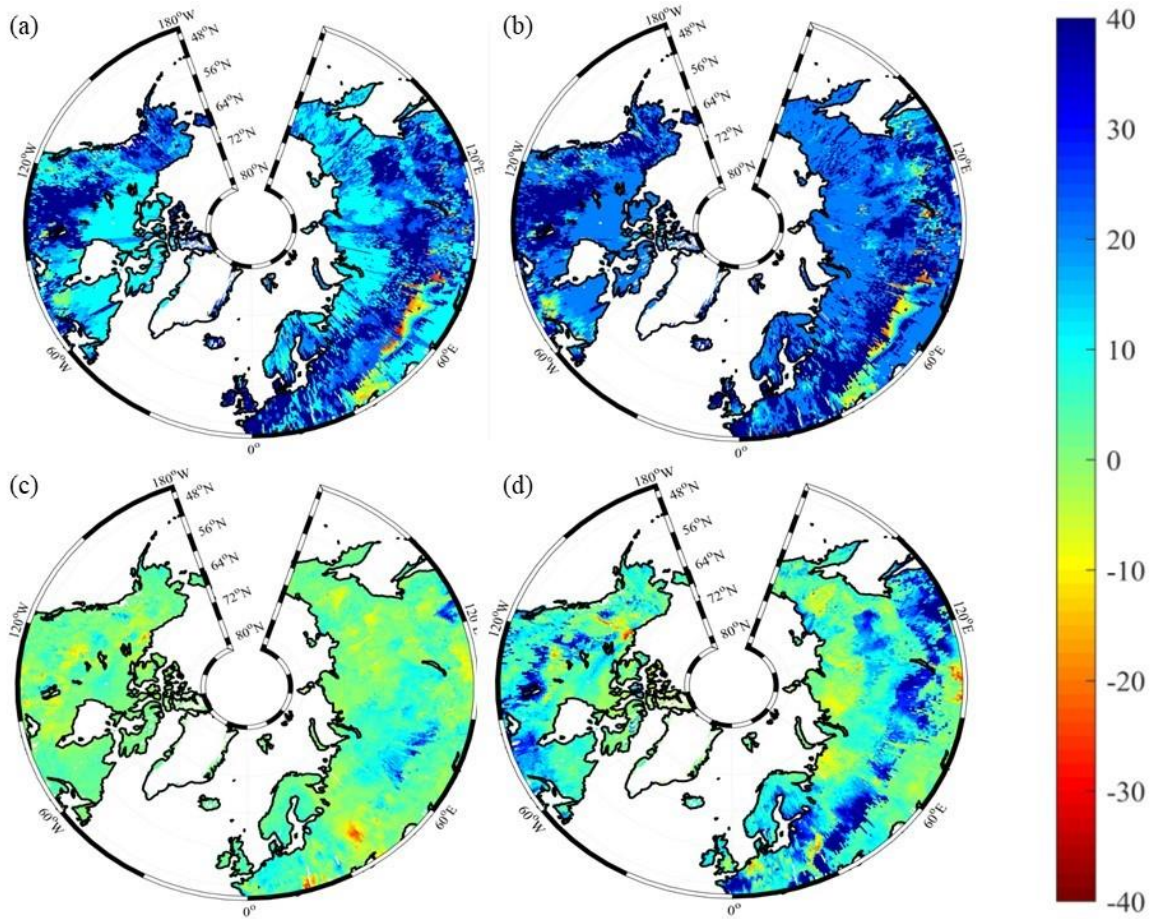
937

938

939

940

941



942

943 Figure 10. Spatial distribution of NEP simulated by TEM_Moss for the periods (a) 1900–1950,
 944 (b) 1951–2000, and by TEM 5.0 for the periods (c) 1900–1950, (d) 1951–2000. Positive values
 945 of NEP represent sinks of CO₂ into terrestrial ecosystems, while negative values represent
 946 sources of CO₂ to the atmosphere.

947

948

949

950

951

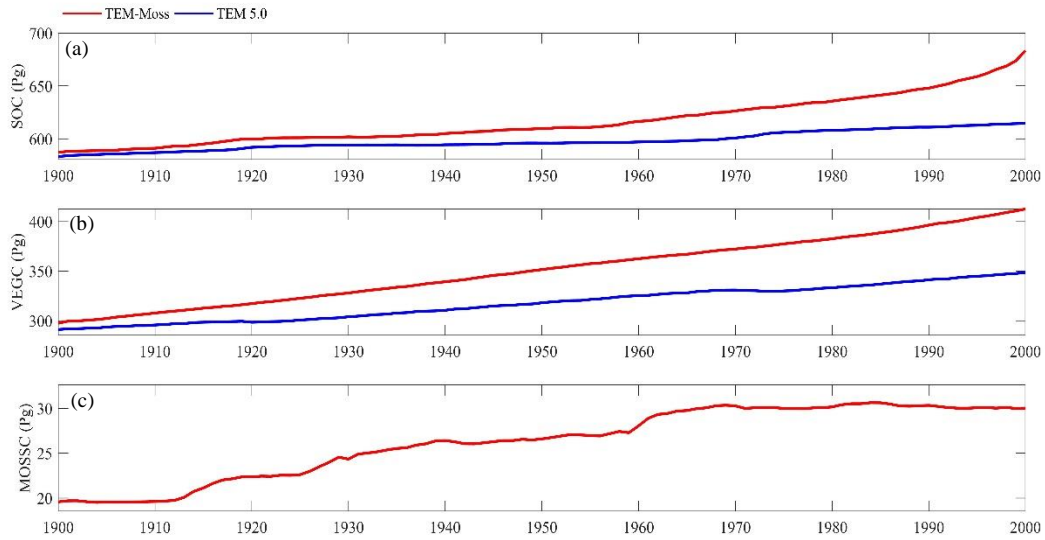
952

953

954

955

956



957

958 Figure 11. Simulated annual soil organic carbon (SOC, a), vegetation carbon (VEGC, b), and
 959 moss carbon (MOSSC, c) during the 20th century by TEM_Moss and TEM 5.0.

960

961

962

963

964

965

966

967

968

969

970

971

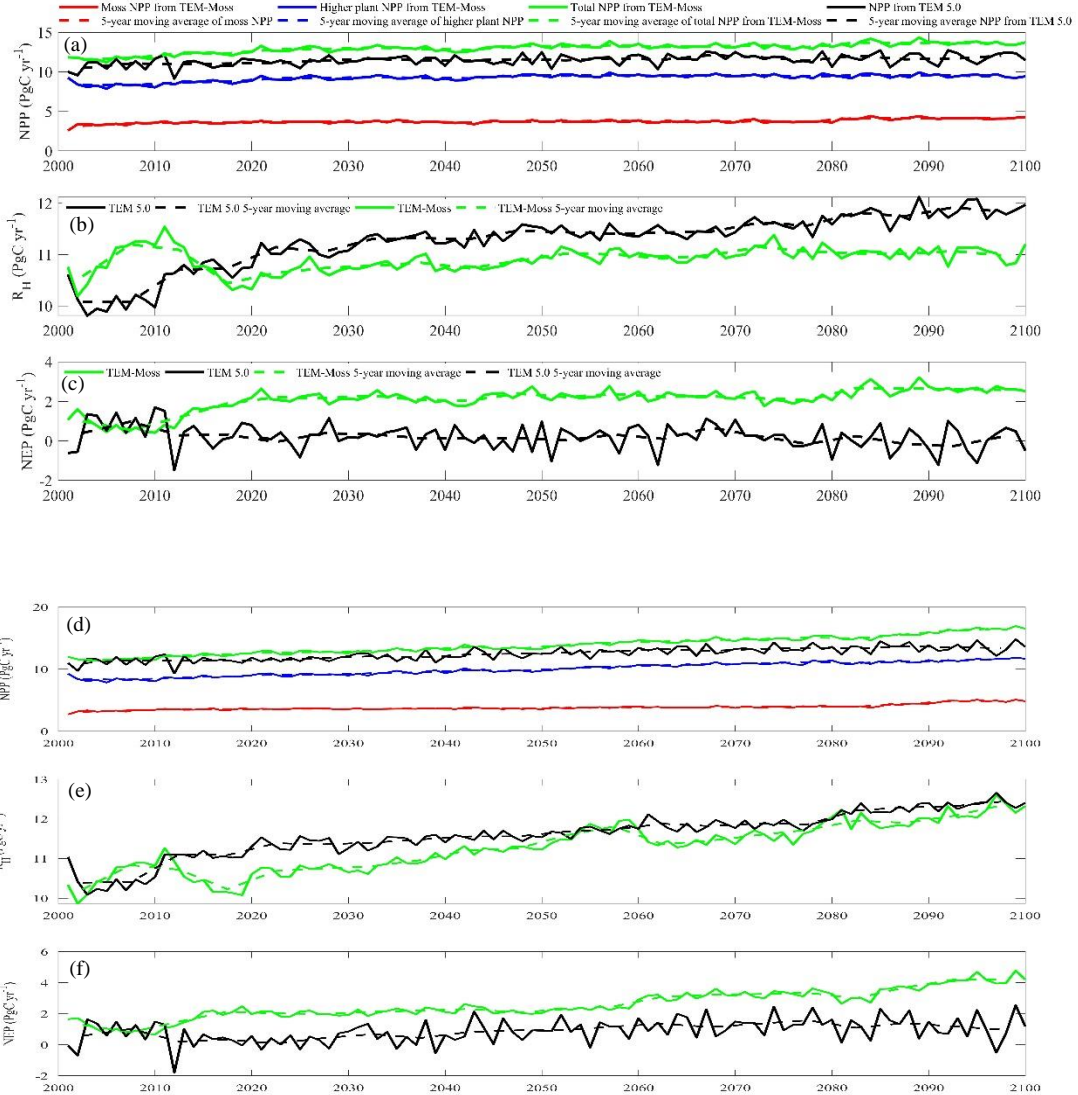
972

973

974

975

976



977

978

979

980

981

982

983

984

985

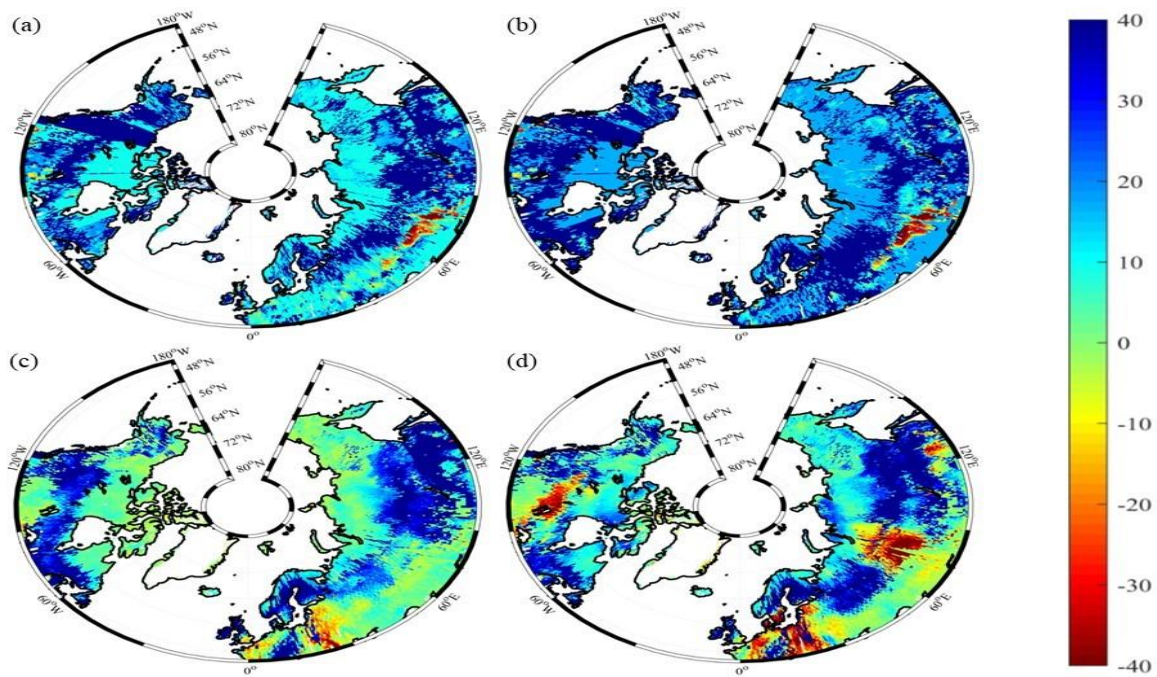
986

987

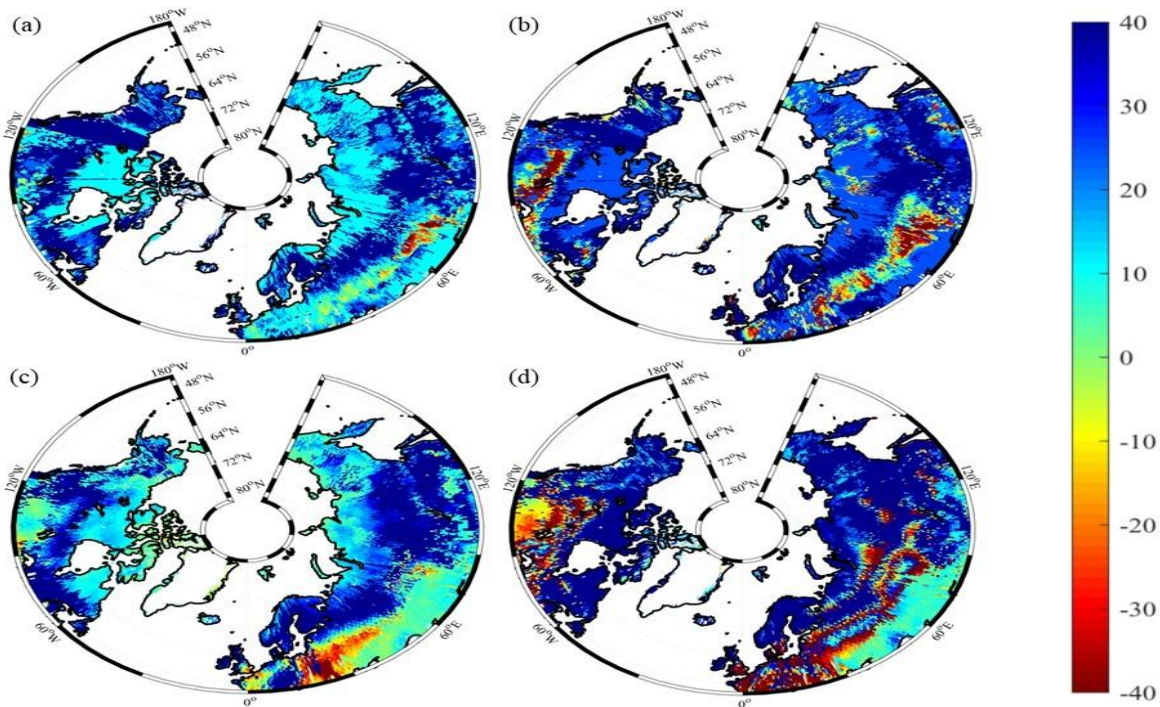
988

Figure 12. Predicted changes in carbon fluxes: annual net primary production (NPP, (a, d)), heterotrophic respiration (R_H , (b, e)), and net ecosystem production (NEP, (c, f)) during the 21st century under RCP 2.6 scenario (a, b, c, upper panel) and RCP 8.5 scenario (d, e, f, bottom panel) by TEM_Moss and TEM 5.0.

989



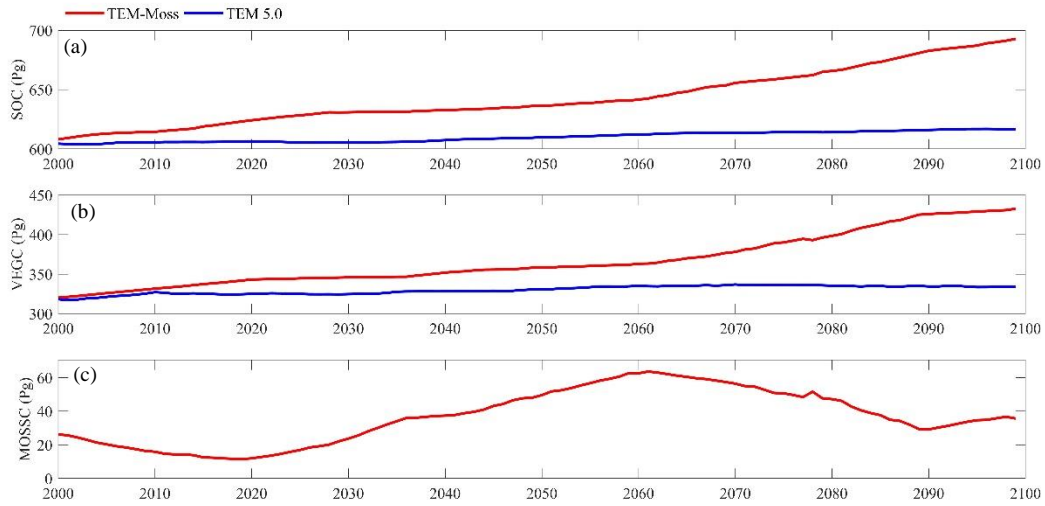
990



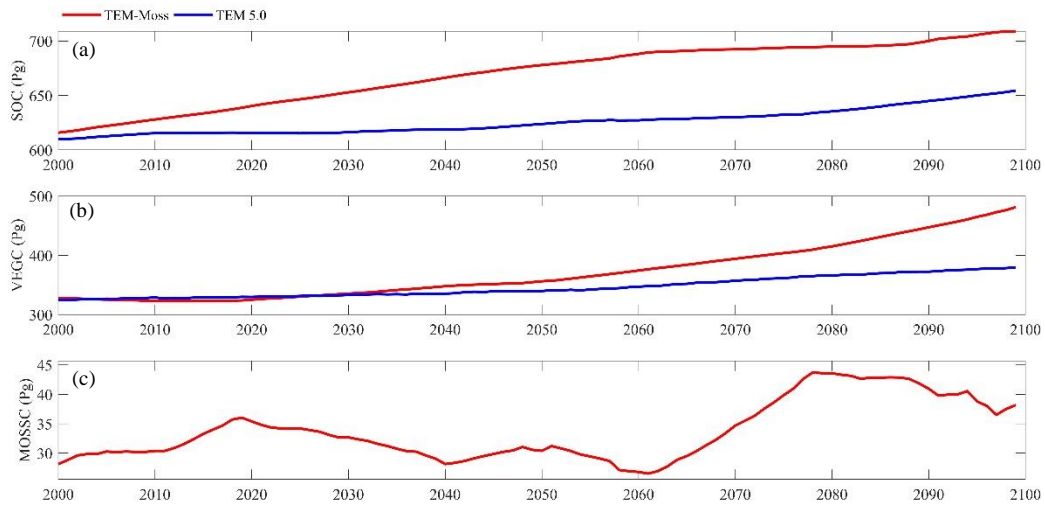
991

992 Figure 13. Spatial distribution of NEP simulated for the periods (a) 2000–2050, (b) 2051–2099
993 by TEM_Moss, and by TEM 5.0 (c, d) during the 21st century under RCP 2.6 scenario (upper
994 panel) and RCP 8.5 scenario (bottom panel). Positive values of NEP represent sinks of CO₂ into
995 terrestrial ecosystems, while negative values represent sources of CO₂ to the atmosphere.

996



997



998

999 Figure 14. Simulated annual soil organic carbon (SOC, a), vegetation carbon (VEGC, b), and
 1000 moss carbon (MOSSC, c) during the 21st century by TEM_Moss and TEM 5.0 under RCP 2.6
 1001 scenario (upper panel) and RCP 8.5 scenario (bottom panel).

1002

1003

1004

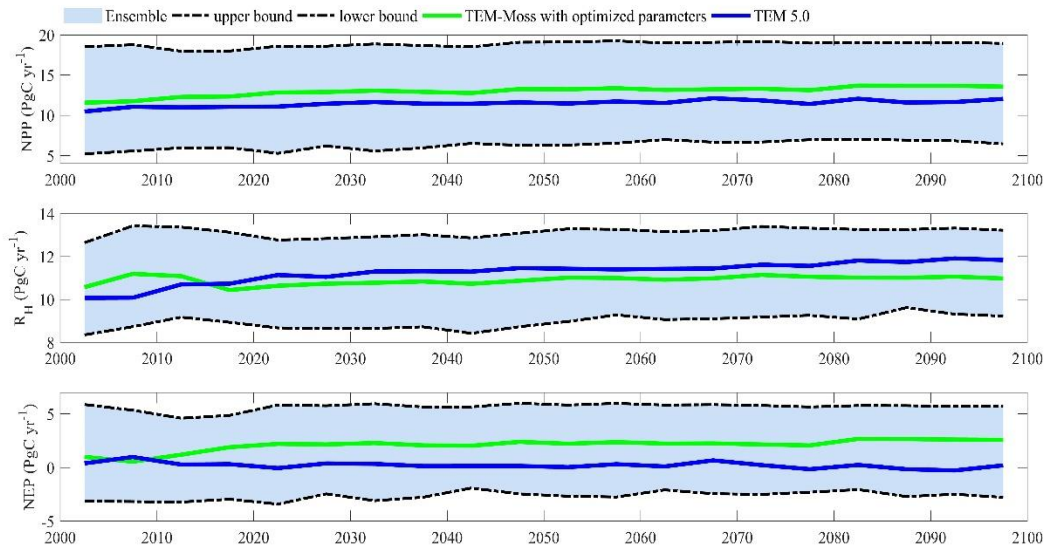
1005

1006

1007

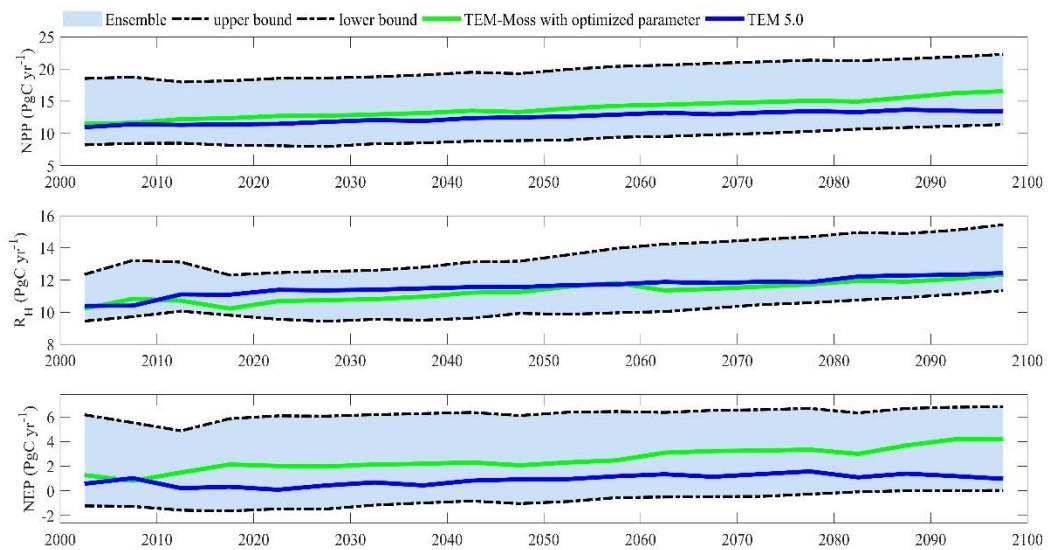
1008

1009 (a)



1010

1011 (b)



1012

1013 Figure 15. 5-year moving average plots for carbon fluxes under the (a) RCP 2.6 scenario and (b)
1014 RCP 8.5 scenario. The blue area represents the upper and lower bounds of simulations.

1015

1016

1017

1018 **Table 1. Parameters associated with moss activities in TEM_Moss**

Parameters	Units	descriptions	Parameter range (value)	references
C_{\max}	$\text{gC m}^{-2} \text{mon}^{-1}$	maximum rate of C assimilation	[50,500]	Launiainen et al. (2015); Williams & Flanagan (1998)
b	$\mu\text{mol m}^{-2} \text{s}^{-1}$	Light half-saturation level	[5, 150]	Launiainen et al. (2015); Raich et al. (1991)
T_{\min}	$^{\circ}\text{C}$	minimum temperature	[-10, 10]	Frolking et al. (1996); Raich et al. (1991)
T_{\max}	$^{\circ}\text{C}$	maximum temperature	[30, 80]	Frolking et al. (1996); Raich et al. (1991)
T_{opt}	$^{\circ}\text{C}$	optimal temperature	[15, 30]	Frolking et al. (1996); Raich et al. (1991)
w_{\min}	mm	minimum water content for moss photosynthesis	[0.5, 15]	Frolking et al. (1996); Launiainen et al. (2015)
w_{\max}	mm	maximum water content for moss photosynthesis	[150, 380]	Frolking et al. (1996); Launiainen et al. (2015)
w_{opt}	mm	optimal water content for moss photosynthesis	[10, 150]	Frolking et al. (1996); Zhuang et al. (2002)
k_m	$\mu\text{L/L}$	CO_2 concentration half-saturation level	[50, 500]	Zhuang et al. (2002); Raich et al. (1991)
$R_{10, m}$	$\text{gC m}^{-2} \text{mon}^{-1}$	moss respiration rate at 10 $^{\circ}\text{C}$	[0,40]	Frolking et al. (1996); Launiainen et al. (2015)
$Q_{10, m}$	-	moss respiration temperature sensitivity	[1.5, 2.5]	Frolking et al. (1996); Launiainen et al. (2015)
$w_{\text{opt}, r}$	mm	optimal water content for moss respiration	[10, 150]	Frolking et al., 1996; Zhuang et al. (2002)
$c_{\text{fall}, m}$	$\text{g}^{-1}\text{g}^{-1} \text{mon}^{-1}$	constant proportion for carbon litterfall from moss	[0.001, 0.01]	Zhuang et al. (2002); Raich et al. (1991)
N_{\max}	$\text{gN m}^{-2} \text{mon}^{-1}$	maximum rate of N uptake by mosses	[0.1,5]	Zhuang et al. (2002); Raich et al. (1991)
k_n	g m^{-2}	Half-saturation constant for N uptake by moss	1.0	Zhuang et al. (2002); Raich et al. (1991)
A_m	-	relative allocation of effort to C vs. N uptake	[0,1]	Raich et al. (1991)
w_f	mm	moss field capacity	[10, 80]	Frolking et al. (1996); Raich et al. (1991)
$n_{\text{fall}, m}$	$\text{g}^{-1}\text{g}^{-1} \text{mon}^{-1}$	constant proportion for nitrogen litterfall from moss	[0.001, 0.01]	Zhuang et al. (2002); Raich et al. (1991)
D_m	mm	Moss thickness	[0, 100]	Zhuang et al. (2002)

Table 2. Site description and measured NEP data used to calibrate TEM_Moss

Site Name	Location (Longitude (degrees) /Latitude (degrees))	Elevation (m)	Vegetation type	Description	Data range	Citations
Univ. of Mich. Biological Station	84.71W 45.56 N	234	Temperate deciduous forest	Located within a protected forest owned by the University of Michigan. Mean annual temperature is 5.83° C with mean annual precipitation of 803mm	01/2005- 12/2006	Gough et al. (2013)
Howland Forest (main tower)	68.74W 45.20N	60	Temperate coniferous forest	Closed coniferous forest, minimal disturbance.	01/2004- 12/2004	Davidson et al. (2006)
UCI-1964 burn site	98.38W 55.91N	260	Boreal forest	Located in a continental boreal forest, dominated by black spruce trees, within the BOREAS northern study area in central Manitoba, Canada.	01/2004- 10/2005	Goulden et al. (2006)
KUOM Turfgrass Field	93.19W 45.0N	301	Grassland	A low-maintenance lawn consisting of cool-season turfgrasses.	01/2006- 12/2008	Hiller et al. (2010)
Atqasuk	157.41W 70.47N	15	Wet tundra	100 km south of Barrow, Alaska. Variety of moist-wet coastal sedge tundra, and moist-tussock tundra surfaces in the more well-drained upland.	01/2005- 12/2006	Oechel et al. (2014);
Ivotuk	155.75W 68.49N	568	Alpine tundra	300 km south of Barrow and is located at the foothill of the Brooks Range and is classified as tussock sedge, dwarf-shrub, moss tundra.	01/2004- 12/2004	McEwing et al. (2015)

Table 3. Site description and measured NEP data used to validate TEM_Moss

Site Name	Location (Longitude (degrees) /Latitude (degrees))	Elevation (m)	Vegetation type	Description	Data range	Citations
Bartlett Experimental Forest	71.29W/ 44.06N	272	Temperate deciduous forest	Located within the White Mountains National Forest in north-central New Hampshire, USA, with mean annual temperature of 5.61 °C and mean annual precipitation of 1246mm.	01/2005- 12/2006	Jenkins et al. (2007); Richardson et al. (2007);
Howland Forest (main tower)	68.74W/ 45.20N	60	Temperate coniferous forest	Closed coniferous forest, minimal disturbance.	01/2003- 12/2003	Davidson et al. (2006)
UCI-1964 burn site	98.38W/ 55.91N	260	Boreal forest	Located in a continental boreal forest, dominated by black spruce trees, within the BOREAS northern study area in central Manitoba, Canada.	01/2002- 12/2003	Goulden et al. (2006)
Brookings	96.84W/ 44.35N	510	Grassland	Located in a private pasture, belonging to the Northern Great Plains Rangelands, the grassland is representative of many in the north central United States, with seasonal winter conditions and a wet growing season.	01/2005- 12/2006	Gilmanov et al. (2005)
Atqasuk	157.41W/ 70.47N	15	Wet tundra	100 km south of Barrow, Alaska. Variety of moist-wet coastal sedge tundra, and moist-tussock tundra surfaces in the more well-drained upland.	01/2003- 12/2004	Oechel et al. (2014);
Ivotuk	155.75W/ 68.49N	568	Alpine tundra	300 km south of Barrow and is located at the foothill of the Brooks Range and is classified as tussock sedge, dwarf-shrub, moss tundra.	01/2005- 12/2005	McEwing et al. (2015)

Table 4. Site description and measured volumetric soil moisture data used to validate TEM_Moss

Site	Location (Longitude (degrees) /Latitude (degrees))	Elevation (m)	Vegetation type	Data range	Citations
US-Ivo	155.75W/ 68.49N	579	Alpine tundra	01/2015- 12/2016	Oechel & Kalhori (2018)
BOREAS NSA-OBS	98.48W/ 55.88N	259	Boreal forest	07/1995- 06/1997	Stangel & Kelly (1999)
NL-Loo	5.74E/ 52.17N	25	Temperate coniferous forest	05/1997- 12/1998	Falge et al. (2005)
DK-Sor	11.64E/ 55.49N	40	Temperate deciduous forest	01/1997- 12/1999	Falge et al. (2005)
US-Bkg	96.84W/ 44.35N	510	Grasslands	01/2005- 12/2006	Gilmanov et al. (2005)
US-Atq	157.41W/ 70.47N	25	Wet tundra	01/2015- 12/2016	Oechel & Kalhori (2018)

Table 5. Site description and measured soil temperature at 5cm depth data used to validate TEM_Moss

Site	Location (Longitude (degrees) /Latitude (degrees))	Elevation (m)	Vegetation type	Data range	Citations
US-Ivo	155.75W/ 68.49N	579	Alpine tundra	01/2015- 12/2016	Oechel & Kalhori (2018)
BOREAS NSA-OBS	98.48W/ 55.88N	259	Boreal forest	01/1995- 12/1998	Stangel & Kelly (1999)
US-Ho1	68.74W/ 45.2N	60	Temperate coniferous forest	01/1996- 12/1997	Falge et al. (2005)
BE-Vie	6.0E/ 50.3N	493	Temperate deciduous forest	01/1997- 12/1998	Falge et al. (2005)
US-Bkg	96.84W/ 44.35N	510	Grasslands	01/2005- 12/2006	Gilmanov et al. (2005)
US-Atq	157.41W/ 70.47N	25	Wet tundra	01/2015- 12/2016	Oechel & Kalhori (2018)

Table 6. Model validation statistics for TEM_Moss and TEM 5.0 at six sites with NEP data

Site Name	Vegetation type	Models	Intercept	Slope	R-square	Adjusted R-square	RMSE	p-value
Ivotuk	Alpine tundra	TEM_Moss	0.46	0.61	0.72	0.70	3.57	<0.001
		TEM 5.0	-0.22	0.75	0.43	0.41	5.88	0.02
UCI-1964 burn site	Boreal forest	TEM_Moss	-0.13	1.01	0.91	0.90	8.33	<0.001
		TEM 5.0	-2.45	1.29	0.75	0.74	20.1	<0.001
Howland Forest (main tower)	Temperate coniferous forest	TEM_Moss	-1.28	1.05	0.83	0.81	19.69	<0.001
		TEM 5.0	-2.22	0.97	0.62	0.61	31.23	0.002
Bartlett Experimental Forest	Temperate deciduous forest	TEM_Moss	-0.49	1.03	0.94	0.94	19.06	<0.001
		TEM 5.0	-2.49	1.04	0.91	0.89	23	<0.001
Brookings	Grassland	TEM_Moss	0.36	1.02	0.85	0.84	8.95	<0.001
		TEM 5.0	2.58	0.75	0.62	0.6	13.07	<0.001
Atqasuk	Wet tundra	TEM_Moss	-0.36	0.97	0.84	0.83	5.13	<0.001
		TEM 5.0	1.99	0.75	0.75	0.74	6.56	<0.001

Table 7. Model validation statistics for TEM_Moss and TEM 5.0 at six sites with volumetric soil moisture data

Site ID	Vegetation type	Models	Intercept	Slope	R-square	Adjusted R-square	RMSE	p-value
US-Ivo	Alpine tundra	TEM_Moss	8.56	0.34	0.74	0.72	20.8	<0.001
		TEM 5.0	10.67	0.29	0.64	0.62	21.76	<0.001
BOREAS NSA-OBS	Boreal forest	TEM_Moss	10.71	0.51	0.52	0.51	11.1	<0.001
		TEM 5.0	16.47	0.43	0.32	0.31	11.96	<0.001
NL-Loo	Temperate coniferous forest	TEM_Moss	0.47	0.82	0.83	0.81	4.0	<0.001
		TEM 5.0	3.75	0.72	0.49	0.48	4.5	<0.001
DK-Sor	Temperate deciduous forest	TEM_Moss	1.39	0.86	0.67	0.65	3.65	<0.001
		TEM 5.0	10.41	0.54	0.4	0.39	4.06	<0.001
US-Bkg	Grassland	TEM_Moss	5.64	0.8	0.51	0.49	6.05	<0.001
		TEM 5.0	22.24	0.41	0.21	0.2	7.34	0.027
US-Atq	Wet tundra	TEM_Moss	7.76	0.77	0.87	0.85	7.38	<0.001
		TEM 5.0	6.74	0.68	0.85	0.84	7.63	<0.001

Table 8. Model validation statistics for TEM_Moss and TEM 5.0 at six sites with soil temperature at 5cm depth data

Site ID	Vegetation type	Models	Intercept	Slope	R-square	Adjusted R-square	RMSE	p-value
US-Ivo	Alpine tundra	TEM_Moss	-0.34	1.16	0.83	0.82	2.54	<0.001
		TEM 5.0	0.54	1.36	0.75	0.73	3.94	<0.001
BOREAS NSA-OBS	Boreal forest	TEM_Moss	-0.05	0.91	0.9	0.88	2.24	<0.001
		TEM 5.0	0.27	0.81	0.84	0.82	2.9	<0.001
US-Ho1	Temperate coniferous forest	TEM_Moss	0.7	0.95	0.81	0.79	2.93	<0.001
		TEM 5.0	-0.06	0.99	0.77	0.76	3.41	<0.001
BE-Vie	Temperate deciduous forest	TEM_Moss	0.57	0.92	0.83	0.81	1.82	<0.001
		TEM 5.0	1.88	0.85	0.69	0.68	2.56	<0.001
US-Bkg	Grassland	TEM_Moss	0.17	0.87	0.91	0.89	2.87	<0.001
		TEM 5.0	-0.01	0.91	0.89	0.87	3.04	<0.001
US-Atq	Wet tundra	TEM_Moss	1.36	0.86	0.84	0.82	3.63	<0.001
		TEM 5.0	4.33	0.99	0.75	0.74	6.17	<0.001

Table 9. Average annual NPP, R_H and NEP (as Pg C per year) during the 20th century estimated by two models.

Average annual carbon fluxes (PgC yr ⁻¹)		TEM_Moss	TEM 5.0	Difference	Moss NPP/ Vascular plants NPP
NPP	Moss NPP	1.69	-	-	21.3%
	Vascular plants NPP	7.93	8.8	-	
	Total NPP	9.6	8.8	0.8	
R_H		7.38	7.91	-0.53	
NEP		2.22	0.89	1.33	

Table 10. Increasing of SOC, vegetation carbon (VGC), and moss carbon (MOSSC) from 1900 to 2000, and total carbon storage during the 20th century predicted by two models.

Models	Carbon pools	Carbon pool amounts in 1900/2000 (units: Pg)	Changes in carbon pools during the 20 th century (units: Pg)
TEM_Moss	SOC	587.1/683.4	96.3
	VEGC	297.5/412.7	115.2
	MOSSC	19.6/30	10.4
	Total	904.2/1126.1	221.9
TEM 5.0	SOC	583.2/614.9	31.7
	VEGC	291.1/348.6	57.5
	Total	874.3/963.5	89.2

Table 11. Average annual NPP, R_H and NEP (as Pg C per year) during the 21st century estimated by two models under (a) RCP 8.5 scenario and (b) RCP 2.6 scenario.

(a)

Average annual carbon fluxes (PgC yr ⁻¹)		TEM_Moss	TEM 5.0	Difference	Moss NPP/ Vascular plants NPP
NPP	Moss NPP	3.84	-	-	38.4%
	Vascular plants NPP	10	12.53	-	
	Total NPP	13.84	12.53	1.31	
R_H		11.28	11.54	-0.21	
NEP		2.56	0.99	1.57	

(b)

Average annual carbon fluxes (PgC yr ⁻¹)		TEM_Moss	TEM 5.0	Difference	Moss NPP/ Vascular plants NPP
NPP	Moss NPP	3.74	-	-	40.5%
	Vascular plants NPP	9.24	11.52	-	
	Total NPP	12.98	11.52	1.46	
R_H		10.91	11.24	-0.33	
NEP		2.07	0.28	1.79	

Table 12. Increasing of SOC, vegetation carbon (VGC), and moss carbon (MOSSC) from 1900 to 2000, and total carbon storage during the 21st century predicted by two models under (a) RCP 2.6 scenario and (b) RCP 8.5 scenario.

(a)

Models	Carbon pools	Carbon pool amounts in 2000/2099 (units: Pg)	Changes in carbon pools during the 21 st century (units: Pg)
TEM_Moss	SOC	608.1/692.8	84.7
	VEGC	320.2/432.8	112.6
	MOSSC	26.2/35.6	9.4
	Total	954.5/1161.2	206.7
TEM 5.0	SOC	604.4/616.5	12.1
	VEGC	318.2/333.7	15.5
	Total	922.6/950.2	27.6

(b)

Models	Carbon pools	Carbon pool amounts in 2000/2099 (units: Pg)	Changes in carbon pools during the 21 st century (units: Pg)
TEM_Moss	SOC	615.9/708.4	92.5
	VEGC	327.8/481.4	153.6
	MOSSC	28.1/38.2	10.1
	Total	971.8/1228.0	256.2
TEM 5.0	SOC	610.2/654.4	44.2
	VEGC	324.9/379.4	54.5
	Total	935.1/1033.8	98.7